Chapter 8 A New Simplified Analytical Internal Mechanics Model for Ship Side Structure Damage

8.1 Introduction

In chapter 5-7, the ALE FE method is proved to be suitable to predict oil tanker side structure damage response taking account of the fluid-structure interaction of the surrounding water and oil in cargo tank. However, this approach is not design oriented since it requires enormous modeling efforts and computing time. For a large commercial vessel, a few days of CPU time on a workstation are required for simulating a collision or grounding accident. Modeling requires, at least, another one to three months. From the viewpoint of designers, such analysis is far from being feasible. The cost of this analysis is prohibitively high. Proper assessment needs some special techniques, which are not transparent to most naval architects. In this regard, simplified analytical methods are highly preferable.

The purpose of this chapter is to develop a new simplified analytical internal mechanic model for calculating the impact force and the dissipated energy caused by the side structure damage, transverse vibration and global motions of struck ship. The energy induced by the transverse vibration and global motions (including surge, sway, roll, pitch and yaw) are taken into account. Series calculations of ship-ship collisions at different striking velocities are discussed and the critical striking velocity is obtained. Compared with existing results obtained by FEM simulation in time domain, the validation of the applicability of new simplified analytical method is employed. Application of new simplified method to mean oil outflow estimation is performed in section 8.6. Conclusions are collected in section 8.7

8.2 Previous Simplified Model for Ship Side Structure Damage

The simplified model for side structure damage developed by Wang et al (2000) is basically an energy method. The idea is that the work of an external force must equal the plastic deformed energy dissipation in the structure. The progressive failure model of a double hull structure is can be seen in Fig. 8.1. Damage of the side structure is a progressive process. With indentation increases further and further, more and more structures become involved. The resistance load increases because of the large volume of

damaged structures. The primary structural failure modes are identified and idealized as penetration of plate, denting of web and tearing of plate.

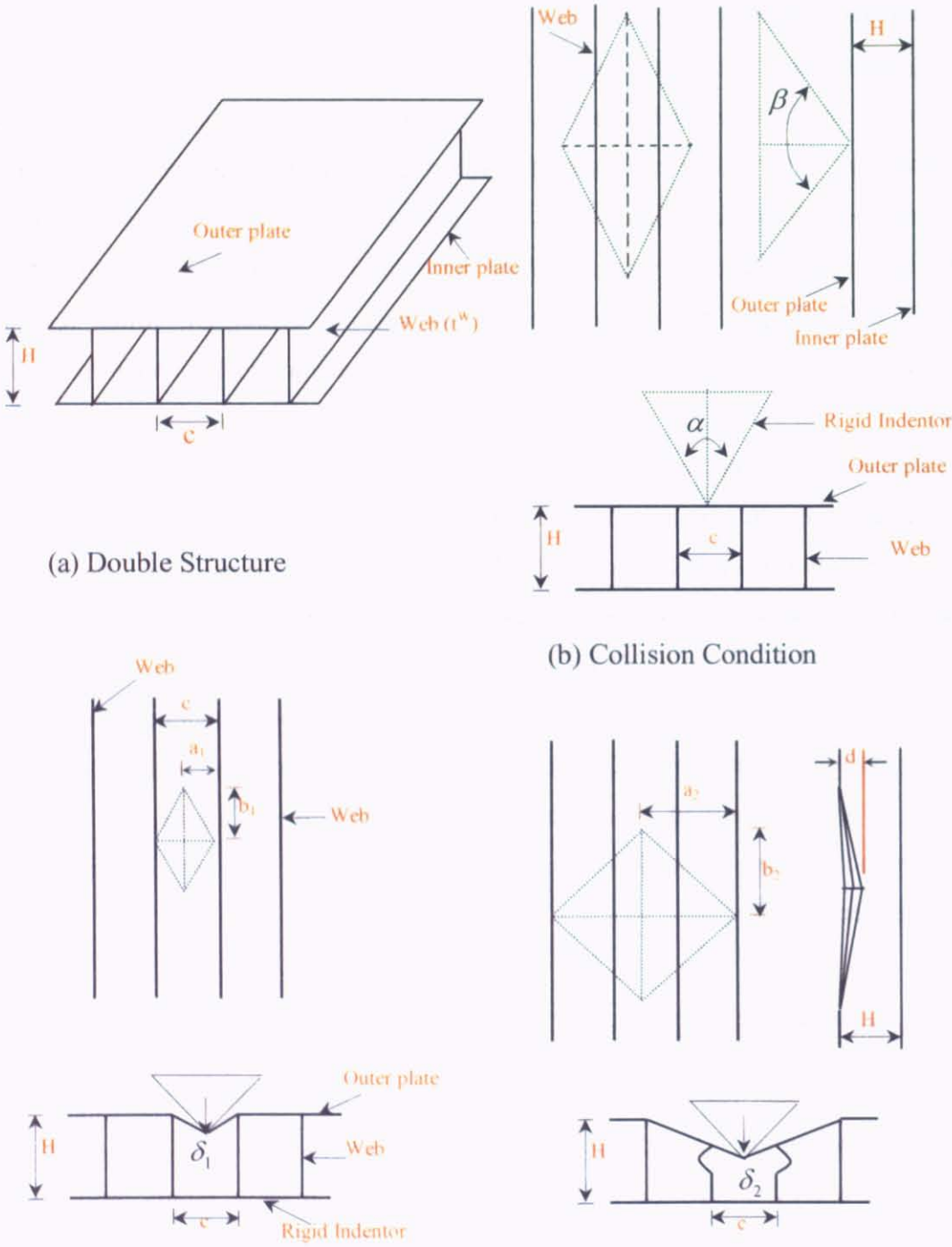

(a) Double Structure

(b) Collision Condition

(c) Initial Deformation

(d) Spread of Deformation to Neighbouring Webs

Fig. 8.1 Progressive failure model of a double hull structure

Because concentrated load is usually assumed in researches in side collision situation, the load-carrying capacity of penetration of the side shell is discussed. The rigid bow forces the plasticity spread the whole extent of the plate. After wrapped round the bow, this part of material is assumed to remain rigid. At a given finite deflection, the material within the boundary and wrapped part of plate are assumed to be yielding uniformly. By application of theoretical plasticity methods and minimization of the energy dissipation, the load-carrying capacity of penetration of the side shell is given by:

$$F_P = 2N_0 \frac{a_1^2 + b_1^2}{a_1 b_1} \delta_1 \qquad N_0 = \sigma_0 t \tag{8.1}$$

Where σ_0 is material flow stress, t is thickness of shell side plate

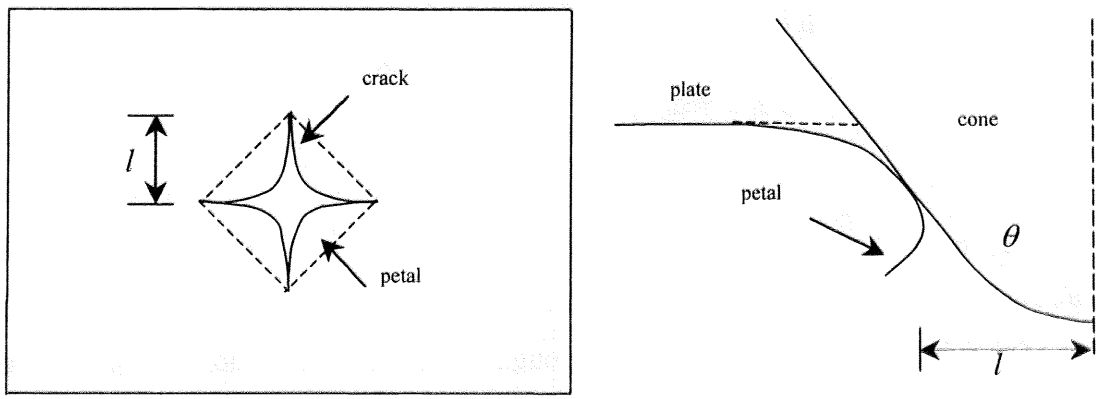

Fig. 8.2 Model for ruptured plate

The plate crack process, as shown in Fig. 8.2, is similar to the plate tearing mechanism. This process involves very large stretching in the vicinity of the striker (bow tip in plate tearing), prominent bending of plate "flaps" or petals remote from striker, and friction. The plate tearing process has been intensively discussed as one of the primary energy absorbing mechanisms in a collision or grounding event. The force needed to drive the crack to a length of l is given by:

$$F_t = 1.51\sigma_0 t^{1.5} l^{0.5} (\sin\theta)^{0.5} (l + \mu / \tan\theta) \tag{8.2}$$

Where l is tearing length, θ is semi-angle of the wedge and μ is friction coefficient.

For a general case, there are n cracks in a perforated plate. It is observed that the petals bend along the lines connecting the crack tips. The perforation process involves

plastic flow near the crack tips, bending of the petals and friction between the cone and the plate. Two adjacent petals form an angle of $(n-2)\pi/n$. When neglecting friction, the force needed to drive one crack to a length of l is given by:

$$P_n = 1.51\sigma_0 t^{1.5} l^{0.5} (\sin((n-2)\pi/2n))^{0.5} \tag{8.3}$$

Where n is the number of cracks in ruptured plate, P_n is in the original plane of the yet not deformed plate.

In order to push the bow into this perforated plate, additional load is required to resist friction. Taking friction into account, the force needed to drive the bow into the perforated plate is given by:

$$F_t = nP_n(\tan\theta + \mu) = 1.51\sigma_0 t^{1.5} l^{0.5} n(\sin((n-2)\pi/2n))^{0.5}(\tan\theta + \mu) \tag{8.4}$$

For denting of webs, the initial phase (before occurrence of buckling) is very short, and the deformation is in the order of plate thickness. Out-of-plane deformation of the web becomes larger and larger as the compression proceeds. If the collision energy is very large, this bulge will eventually evolve into structural folding (see Fig. 8.1). Both bending stress and membrane stress play a role in the energy absorption. If the energy is still not spent, then a new bulge will occur directly behind the fold, and it will develop in a process similar to that of the first-fold. Because web has enough depth in the direction of collision load (compared to the folding length), more than one-fold can be formed. The load-carrying capacity of denting of the web is given by:

$$F_d = 2.32\sigma_0 (2b_1)^{0.33} (t)^{1.67} \tag{8.5}$$

Where $2b_1$ is width of the denting web.

Strain of side shell plate is

$$\varepsilon = \frac{1}{2}\left(\frac{\delta_1}{a_1}\right)^{1/2} \tag{8.6}$$

In simplified analytical model, the failure criterion is that rupture occurs when the strain equals a prescribed critical rupture stain. Here, it is assumed that a plate will rupture if the strain equals 30%.

The plastic deformed energy and friction energy E_{LP} dissipation in the side structure can be expressed as

$$E_{LP} = \int_0^{\delta_u} F_C(\delta) \cdot d\delta \tag{8.7}$$

Here, simplified analytical method is used for the side strength analysis of a 293,000 tonne VLCC, which has a collision barrier side structure, against a collision from 350,000 tonne VLCC. The FEM simulations of the collisions case have been carried out in chapter 6. The stiffened side panel is viewed as a plate structure with equivalent thickness. The total resistance of side structure is obtained by summing all the contributions from plate components that are directly indented by the penetrating bow.

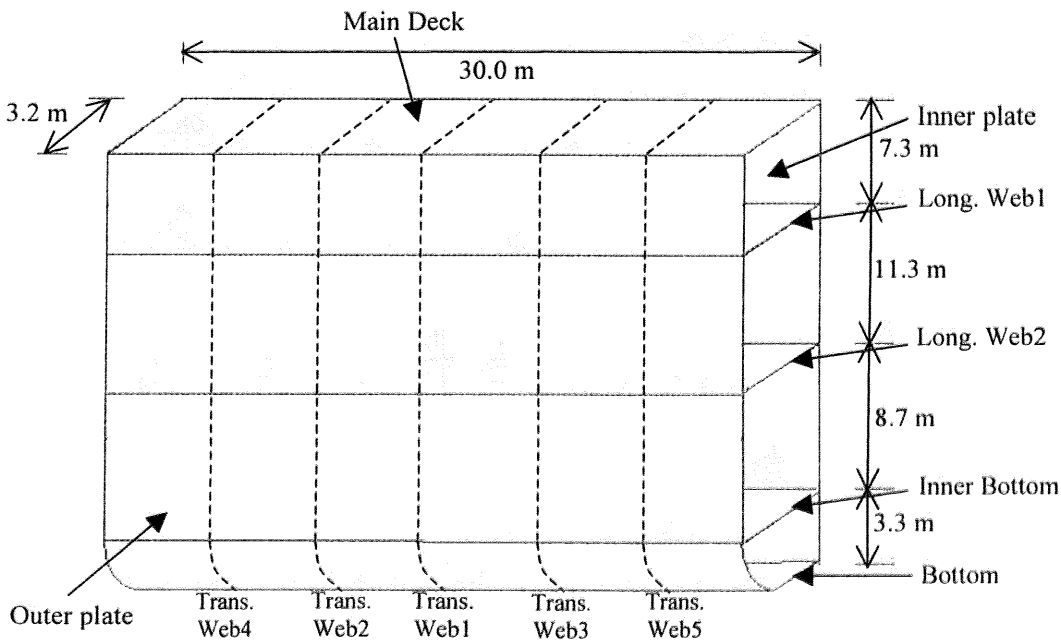

Fig. 8.3 Side structure of struck ship (equivalent thickness is shown)

Brief descriptions of simplified analytical method for side structure of 293,000 tonne VLCC are in the following.

Stage 1 (till the bulb touches inner bottom)

- δ = (0~956) mm
- Penetration of outer plate by bulb, (F_{Pb})
- Denting of transverse web 1, (F_{dT1})
- Total Force, $F_C(\delta) = F_{Pb} + F_{dT1}$

Stage 2 (till the bulb touches transverse web 2, 3)

- δ = (956~1409) mm
- Penetration of outer plate by bulb, (F_{Pb})
- Denting of transverse web 1, (F_{dT1})
- Denting of inner bottom, (F_{dIB})
- Total Force, $F_C(\delta) = F_{Pb} + F_{dT1} + F_{dIB}$

Stage 3 (till the bulb tearing outer plate)

- δ = (1409~1800) mm
- Penetration of outer plate by bulb, (F_{Pb})
- Denting of transverse web 1, 2, 3, ($F_{dT1}, F_{dT2}, F_{dT3}$)
- Denting of inner bottom, (F_{dIB})
- Total Force, $F_C(\delta) = F_{Pb} + F_{dT1} + F_{dT2} + F_{dT3} + F_{dIB}$

Stage 4 (till the stem touches outer plate and main deck)

- δ = (1800~1958) mm
- Tearing of outer plate by bulb, (F_{tb})
- Denting of transverse web 1, 2, 3, ($F_{dT1}, F_{dT2}, F_{dT3}$)
- Denting of inner bottom, (F_{dIB})
- Total Force, $F_C(\delta) = F_{tb} + F_{dT1} + F_{dT2} + F_{dT3} + F_{dIB}$

Stage 5 (till the bulb touches inner plate)

- δ = (1958~3196) mm
- Tearing of outer plate by bulb, (F_{tb})
- Penetration of outer plate by stem, (F_{ps})
- Denting of main deck by stem, (F_{dm})
- Denting of transverse web 1, 2, 3, ($F_{dT1}, F_{dT2}, F_{dT3}$)
- Denting of longitudinal web 1and inner bottom, (F_{dL1}, F_{dIB})
- Total Force, $F_C(\delta) = F_{tb} + F_{ps} + F_{dm} + F_{dT1} + F_{dT2} + F_{dT3} + F_{dL1} + F_{dIB}$

Stage 6 (till the stem tearing of outer plate)

- δ = (3196~3793) mm
- Tearing of outer plate by bulb, (F_{tb})
- Penetration of inner plate by bulb, (F_{pb})
- Penetration of outer plate by stem, (F_{ps})
- Denting of main deck by stem, (F_{dm})
- Denting of transverse web 1, 2, 3, ($F_{dT1}, F_{dT2}, F_{dT3}$)
- Denting of longitudinal web 1and inner bottom, (F_{dL1}, F_{dIB})
- Total Force,

$$F_C(\delta) = F_{tb} + F_{pb} + F_{ps} + F_{dm} + F_{dT1} + F_{dT2} + F_{dT3} + F_{dL1} + F_{dIB}$$

Stage 7 (till the bulb tearing of inner plate)

- δ = (3793~7307) mm
- Tearing of outer plate by bulb, (F_{tb})
- Penetration of inner plate by bulb, (F_{pb})
- Tearing of outer plate by stem, (F_{ts})
- Denting of main deck by stem, (F_{dm})
- Denting of transverse web 1, 2, 3, ($F_{dT1}, F_{dT2}, F_{dT3}$)
- Denting of longitudinal web 1, 2 and inner bottom, ($F_{dL1}, F_{dL2}, F_{dIB}$)
- Total Force,

$$F_C(\delta) = F_{tb} + F_{pb} + F_{ts} + F_{dm} + F_{dT1} + F_{dT2} + F_{dT3} + F_{dL1} + F_{dL2} + F_{dIB}$$

Table 8.1 Force and Energy absorbed at each stage of penetration

Stage	Penetration (mm)	Force(KN)
1	956	2606
2	1409	4085
3	1800	5887
4	1958	18374
5	3196	53662
6	3793	82155
7	7307	223060

The impact force-penetration curve for side structure of 293,000 tonne VLCC till the bulbous bow tearing of inner shell is shown in Fig.8.4. Compared with FEM simulation result, impact force-penetration curve using previous simplified method is underestimated. The main reason is that the overall elastic transverse vibration response and the whole kinetic energy of struck ship (including surge, sway, roll, yaw and pitch motion) are neglected. ALE FEM simulation results of energy components in Fig.8.5 show that the elastic bending energy caused by transverse vibration and global kinetic energy can not be neglected. In the next section, the new simplified analytical model, which is considered the effect of these factors, is proposed.

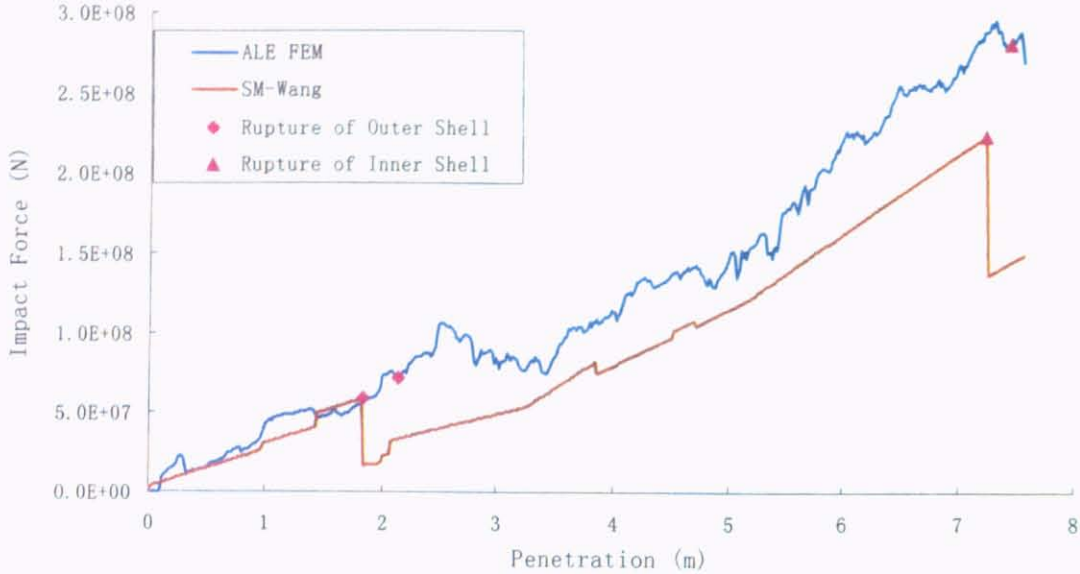

Fig. 8.4 Impact force-penetration curve

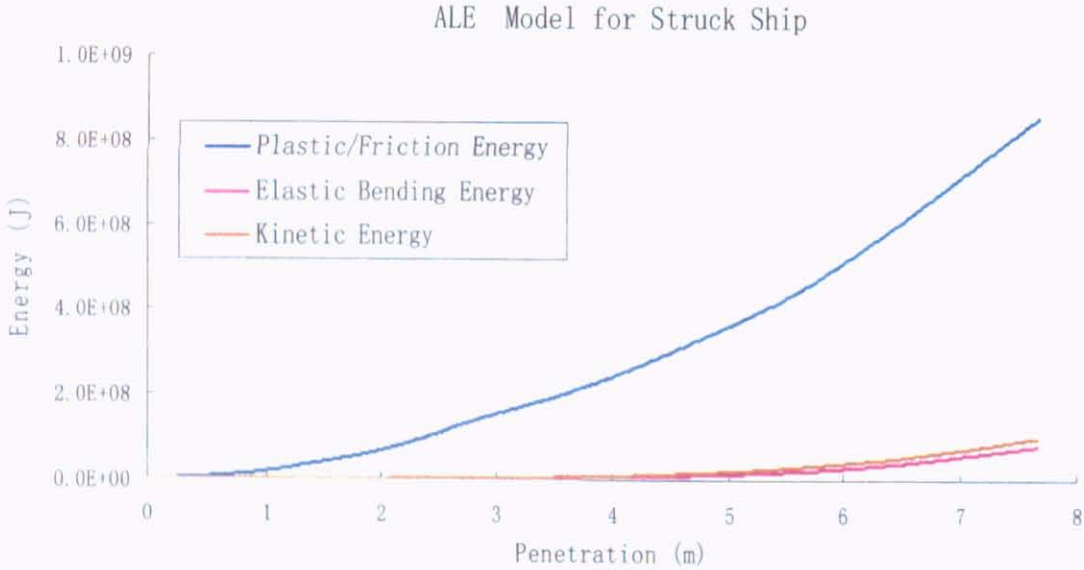

Fig. 8.5 Energy components of FEM simulation result

8.3 New Simplified Analytical Model for Side Structure Damage

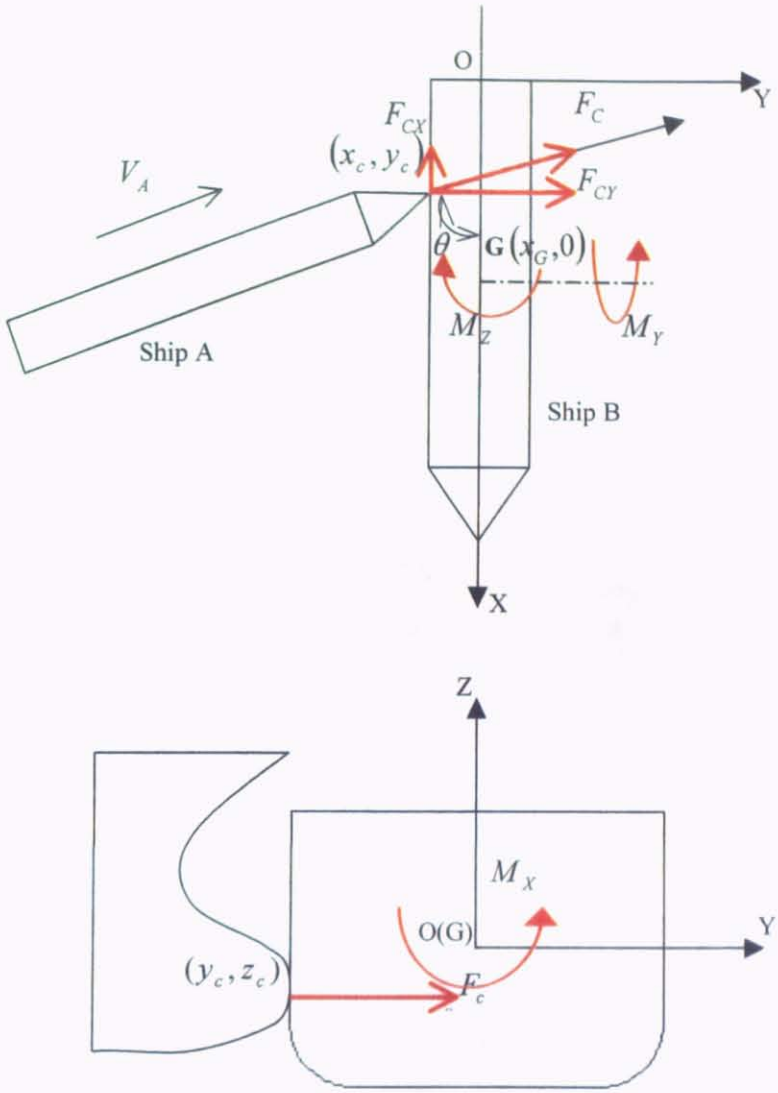

Fig. 8.6 Plan view of arbitrary ship-ship collision

In this section, a new simplified analytical internal mechanics model, which the effects of the overall elastic transverse vibration response, the whole kinetic energy of struck ship(including surge, sway, roll, yaw and pitch motion) on the impact force are also considered, is proposed. As Fig.8.6 shown, the rigid striking ship collides the side structure of struck ship at arbitrary collision location and angle, the impact force will cause the transverse vibration, the roll, yaw, pitch, sway and surge motion of struck ship. For simple, we assume that the striking ship is rigid and the struck ship is standstill.

8.3.1 The Simplified Mechanics Model for Roll Motion of Struck Ship

In section 6.3, ALE FE simulation results show that the roll motion of struck ship is significantly affected the side structure damage process. Endo et al (2004) proposed a simplified spring model to simulate the heave and roll motion in Fig. 8.7.

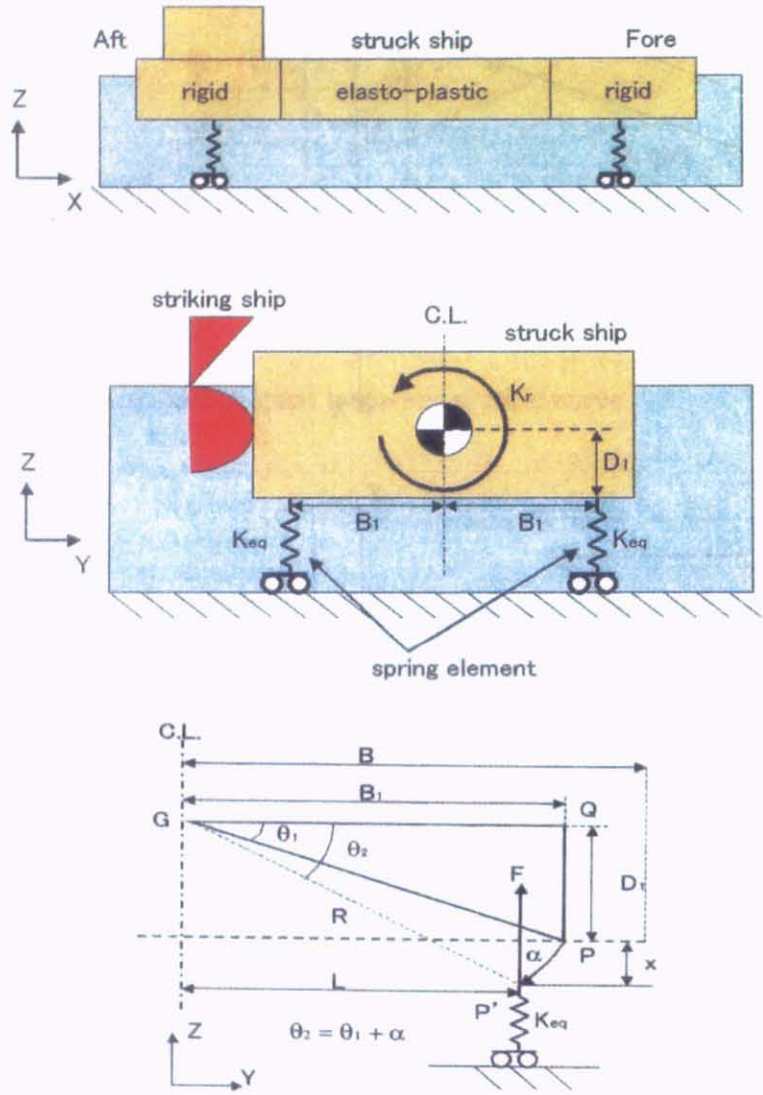

Fig. 8.7 Simplified Spring Model for Roll Motion

The stiffness of 4 spring elements is determined by static restoring moment for the heave motion

$$K_{eq} = \frac{K_h}{4} \tag{8.8}$$

Where K_h is the restoring moment coefficient for heave motion.

The restoring moment using spring model for roll motion is

$$M_{spring} = 4K_{eq} \cdot x \cdot R \cdot \cos(\theta_2) = 4K_{eq} \cdot R^2 \cdot (\sin\theta_2 - \sin\theta_1)\cos\theta_2 \tag{8.9}$$

$$\tan\theta_1 = \frac{D_1}{B_1} \qquad R^2 = D_1^2 + B_1^2 \qquad \theta_2 = \theta_1 + \alpha \tag{8.10}$$

The restoring moment can also be expressed as

$$M_w = K_r \cdot \alpha \tag{8.11}$$

Where α is the roll angle, B_1 is the distance from centre line to spring element, D_1 is the vertical distance from bottom to center of gravity.

Assuming α is small, then $\cos\alpha \approx 1, \sin\alpha \approx \alpha$, $\alpha^2 \approx 0$

$$\sin\theta_2 = \sin(\theta_1 + \alpha) = \sin\theta_1 \cos\alpha + \cos\theta_1 \sin\alpha \approx \sin\theta_1 + \alpha\cos\theta_1$$

$$\cos\theta_2 = \cos(\theta_1 + \alpha) = \cos\theta_1 \cos\alpha - \sin\theta_1 \sin\alpha \approx \cos\theta_1 - \alpha\sin\theta_1 \tag{8.12}$$

The restoring moment using spring model for roll moment can be expressed as

$$M_{spring} = 4K_{eq} \cdot \alpha \cdot R^2 \cdot (\cos\theta_1)^2 = 4K_{eq} \cdot \alpha \cdot B_1^2 \tag{8.13}$$

Finally, we can determine the value of B_1

$$B_1 = \frac{1}{2}\sqrt{\frac{K_r}{K_{eq}}} \tag{8.14}$$

The potential energy of spring can be expressed as

$$E_{Roll} = 4 \times \frac{1}{2} K_{eq} \cdot \Delta x^2 = 2 \times K_{eq} \cdot (D_1^2 + B_1^2)\left[\sin\left(\theta_1 + \frac{F_C \sin\theta \cdot h}{K_r}\right) - \sin\theta_1\right]^2 \tag{8.15}$$

Where h is the vertical distance between the contact point and the centre of gravity.

Here, this spring model is used in FE model to analyze the 293,000 tonne VLCC collided by the 350,000 VLCC (the same ship collision case in section 6.4). The impact force-penetration curve of roll-spring model is presented in Fig. 8.7. Compared with ALE FE model result, the roll-spring model can give good prediction results on the rupture of outside shell plate and inner plate. The spring model can consider the effect of roll motion on the structure damage well.

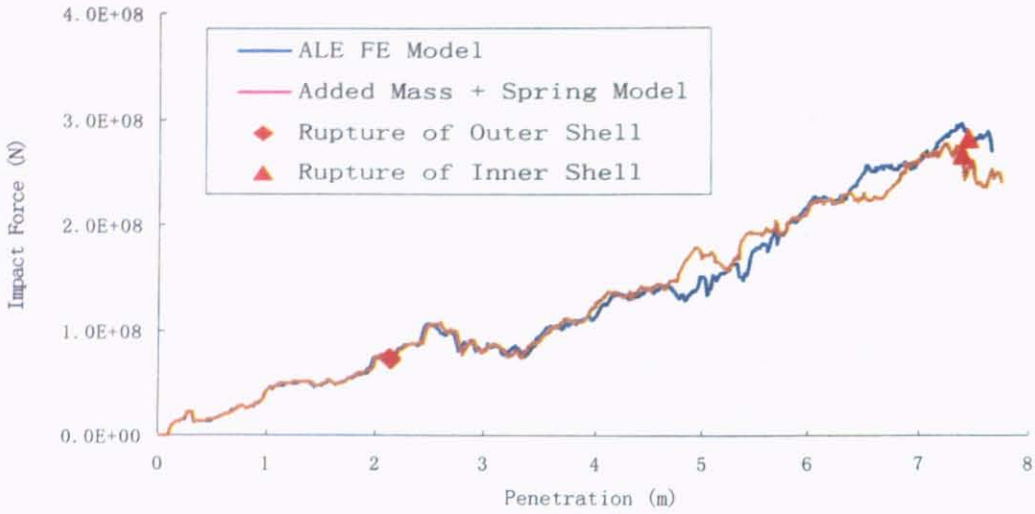

Fig. 8.8 Impact force-penetration curve for roll-spring model

8.3.2 Kinetic Energy of Struck Ship for Surge, Sway, Pitch and Yaw Motion

Motion equations

Here, the transverse displacements of struck ship for surge and sway are denoted by u^b, v^b respectively. The angular displacements of the rotational motion for pitch and yaw are denoted by φ^b, ψ^b respectively.

The motions of struck ship for surge, sway, pitch and yaw can be expressed respectively

$$\left(M^b + A^b{}_{1,1}\right)\ddot{u}^b = -F_C \cos\theta \tag{8.16}$$

$$\left(M^b + A^b{}_{2,2}\right)\ddot{v}^b = F_C \sin\theta \tag{8.17}$$

$$\left(I^b_{yy} + A^b_{5,5}\right)\cdot\ddot{\varphi}^b = -F_C \cos\theta \cdot z_c \tag{8.18}$$

$$\left(I^b_{zz} + A^b_{6,6}\right)\cdot\ddot{\psi}^b = -F_C \sin\theta \cdot \left(x_G - x_c\right) - F_C \cos\theta \cdot \frac{B}{2} \tag{8.19}$$

where M^b, $A^b_{1,1}$ and $A^b_{2,2}$ present mass and added mass for surge, sway motion of struck ship; I^b_{yy} and I^b_{zz} present the moment of inertia with respect to y-axis and z-axis; $A^b_{5,5}$ and $A^b_{6,6}$ present added mass moment of inertia for pitch and yaw.

Calculation of added mass coefficients

For simplicity, the calculation of added mass coefficients in motion equations is given as following.

The hydrodynamic force related to the surge motion of ship is very small compared to sway force. The hydrodynamic forces related to the surge motion cannot be found by strip method. The sectional surge added mass $A_{1,1}$ related to the forward motion is small compared with the mass of the ship. Professor Motora (1969) found it to be $(0.02-0.07)M$. A reasonable assumption may be

$$A_{1,1} = 0.05M \tag{8.20}$$

Many researchers have proposed different methods to evaluate the sectional sway added mass coefficients for ship forms; the pioneer works being that by Lewis F. M. (1929), Tasai F. (1961). The sway hydrodynamic added mass coefficient at infinite frequency using Lewis Two Parameter Conformal Mapping Method to be given by

$$A_{2,2}/M = \frac{2\rho}{\pi}\{D^2 + \frac{16}{3}a_3{}^3\} \tag{8.21}$$

where

$$a_3 = \frac{-c_1 + 3 + (9-2c_1)^{1/2}}{c_1} \tag{8.22}$$

$$c_1 = [3 + \frac{4\sigma_S}{\pi}] + [1 - \frac{4\sigma_S}{\pi}][(H_O - 1)/(H_O + 1)]^2 \tag{8.23}$$

$$H_O = \frac{B}{2D} \qquad \sigma_S = \frac{A_S}{DB} \tag{8.24}$$

B and D is the breadth and draught of cross section, respectively

A_s is wetted area of cross section

The added mass coefficient for the pitch/yaw motion of ship, $A_{5,5}/A_{6,6}$, is (Pedersen et al.,1993)

$$A_{5,5} = 0.21 \cdot I_{yy} \tag{8.25}$$

$$A_{6,6} = 0.21 \cdot I_{zz} \tag{8.26}$$

Kinetic energy for different motions

We assume the external force to a stepwise one of magnitude F_C for a duration δt. Then the velocity/angle velocity of struck ship for surge, sway, pitch and yaw can be expressed respectively

$$\dot{u}^b = \int \ddot{u}^b dt = \int \frac{-F_C \cos\theta}{M^b + A^b{}_{1,1}} dt = \frac{-F_C \cos\theta \cdot \delta t}{M^b + A^b{}_{1,1}} + C_1 \tag{8.27}$$

$$\dot{v}^b = \int \ddot{v}^b \, dt = \int \frac{F_C \sin\theta}{M^b + A^b_{2,2}} dt = \frac{F_C \sin\theta \cdot \delta t}{M^b + A^b_{2,2}} + C_2 \tag{8.28}$$

$$\dot{\varphi}^b = \int \ddot{\varphi}^b dt = \int \frac{-F_C \cos\theta \cdot z_c}{I^b_{yy} + A^b_{5,5}} dt = \frac{-F_C \cos\theta \cdot z_c \cdot \delta t}{I^b_{yy} + A^b_{5,5}} + C_3 \tag{8.29}$$

$$\dot{\psi}^b = \int \ddot{\psi}^b dt = \frac{\left(-F_C \sin\theta \cdot (x_G - x_c) - F_C \cos\theta \cdot \frac{B}{2}\right) \cdot \delta t}{I^b_{zz} + A^b_{6,6}} + C_4 \tag{8.30}$$

At $t = 0$, the constant C_1, C_2, C_3 and C_4 become the initial velocity of struck ship for surge, sway, pitch and yaw motion. During the next time step, C_1, C_2, C_3 and C_4 take the value of $\dot{u}^b, \dot{v}^b, \dot{\varphi}^b$ and $\dot{\psi}^b$ at the end of the previous time step).

The kinetic energy of struck ship for surge motion can be expressed as

$$E_{KSurge} = \frac{1}{2}\left(M^b + A^b_{1,1}\right) \cdot \left(\dot{u}^b\right)^2 = \frac{\left(M^b + A^b_{1,1}\right)}{2} \cdot \left(\frac{-F_C \cos\theta \cdot \delta t}{M^b + A^b{}_{1,1}} + C_1\right)^2 \tag{8.31}$$

The kinetic energy of struck ship for sway motion can be expressed as

$$E_{KSway} = \frac{1}{2}\left(M^b + A^b_{2,2}\right) \cdot \left(\dot{v}^b\right)^2 = \frac{\left(M^b + A^b_{2,2}\right)}{2} \cdot \left(\frac{F_C \sin\theta \cdot \delta t}{M^b + A^b_{2,2}} + C_2\right)^2 \tag{8.32}$$

The kinetic energy of struck ship for pitch motion can be expressed as

$$E_{KPitch} = \frac{1}{2}\left(I^b_{yy} + A^b_{5,5}\right) \cdot \left(\dot{\varphi}^b\right)^2 = \frac{\left(I^b_{yy} + A^b_{5,5}\right)}{2} \cdot \left(\frac{-F_C \cos\theta \cdot z_c \cdot \delta t}{I^b_{yy} + A^b_{5,5}} + C_3\right)^2 \tag{8.33}$$

The kinetic energy of struck ship for yaw motion can be expressed as

$$E_{KYaw} = \frac{1}{2}\left(I_{zz}^{b} + A_{6,6}^{b}\right)\cdot\left(\dot{\psi}^{b}\right)^{2} = \frac{\left(I_{zz}^{b} + A_{6,6}^{b}\right)}{2}\cdot\left(\frac{\left(-F_C \sin\theta\cdot\left(x_G - x_c\right) - F_C \cos\theta\cdot\frac{B}{2}\right)\cdot\delta t}{I_{zz}^{b} + A_{6,6}^{b}} + C_4\right)^{2} \tag{8.34}$$

Total kinetic energy of struck ship for surge, sway, roll, pitch and yaw motion can be expressed as

$$E_{GK} = E_{KSurge} + E_{KSway} + E_{KPitch} + E_{KYaw} + E_{Roll} \tag{8.35}$$

8.3.3 The Hull Transverse Vibratory Response

Impact loading on a ship induces not only the rigid body motions, but also the dynamic bending of the ship hull girder. Dynamic bending covers the hull girder vibration where the cross-sections of the beam remain plane. This allows the modelling of the struck ship hull vibratory as an Euler-Bernoulli beam with free ends and the bending vibration is considered in the plane of the water surface. The transverse hull forced vibration of struck ship can be expressed:

$$EI\frac{\partial^4 v^b(x,t)}{\partial x^4} + C\frac{\partial v^b(x,t)}{\partial t} + \rho\frac{\partial^2 v^b(x,t)}{\partial t^2} = F_C \sin\theta\cdot\delta(x_c) \tag{8.36}$$

$$\rho = \frac{\left(M^b + A_{2,2}^b\right)}{L} \tag{8.37}$$

where M^b and $A_{2,2}^b$ present mass and added mass for sway motion of struck ship; L and EI are the length and flexural stiffness of hull beam; the viscous damping coefficient is denoted C; θ is collision angle and $\delta(x_c)$ is 1 when $x = x_c$ and 0 for other value of x.

The dynamic response of the ship hull girder is a superposition of the responses of the different eigenmodes. The essential operation of the mode-superposition analysis is the transformation from the geometric displacement coordinates to the normal coordinates. The transverse displacement is expressed as

$$v^b(x,t) = \phi(x)\cdot Y(t) \tag{8.38}$$

Where $\phi(x)$ is the natural mode and $Y(t)$ is the normal coordinate

Inserting equation (8.38) into equation (8.36), the equation of $\phi(x)$ can be expressed as

$$EI\frac{d^4\phi(x)}{dx^4} - \rho\omega^2 \cdot \phi(x) = 0 \tag{8.39}$$

$$\beta^4 = \omega^2 \cdot \frac{\rho}{EI} \tag{8.40}$$

The solution of natural mode $\phi(x)$ is

$$\phi(x) = A_1 \sin\beta x + A_2 \cos\beta x + A_3 \sinh\beta x + A_4 \cosh\beta x \tag{8.41}$$

For the boundary condition of free-free-end hull beam vibration

$$\begin{cases} \phi''(0) = \phi'''(0) = 0 \\ \phi''(L) = \phi'''(L) = 0 \end{cases} \tag{8.42}$$

We can get

$$\begin{cases} A_1 = A_3 \\ A_2 = A_4 \\ \cos\beta L \cdot \cosh\beta L = 1 \end{cases} \tag{8.43}$$

$$\beta_k L \approx \left(k + \frac{1}{2}\right)\pi + (-1)^{k+1} \cdot 2e^{-\left(k+\frac{1}{2}\right)\pi} \qquad k \geq 1 \tag{8.44}$$

For $k-th$ natural frequency

$$\omega_k = \beta_k^2 \cdot \sqrt{\frac{EI}{\rho}} \tag{8.45}$$

The normal natural mode

$$\phi_n(x) = A_n\left(\sin\beta_n x + \sinh\beta_n x - \frac{\sin\beta_n L - \sinh\beta_n L}{\cos\beta_n L - \cosh\beta_n L}(\cos\beta_n x + \cosh\beta_n x)\right) \tag{8.46}$$

Furthermore the effect of vibration motion is assumed to be small compared to the rigid body motion, only the first eigenmode is include.

$$\omega_1 = \left(\frac{4.73}{L}\right)^2 \sqrt{\frac{EI}{\rho}} \tag{8.47}$$

$$\phi_1(x) = A_1 \cdot \left(\sin\frac{4.73}{L}x - 1.02\cos\frac{4.73}{L}x + \sinh\frac{4.73}{L}x - 1.02\cosh\frac{4.73}{L}x\right) \tag{8.48}$$

Since $\phi_1(x)$ satisfies the normality condition

$$\int_0^L \rho\phi_1^2(x) = 1 \qquad A_1 = 0.97\sqrt{\frac{1}{\rho L}} \tag{8.49}$$

Then $\phi_1(x)$ can be expressed as

$$\phi_1(x) = \frac{0.97}{\sqrt{\rho L}} \cdot \left(\sin\frac{4.73}{L}x - 1.02\cos\frac{4.73}{L}x + \sinh\frac{4.73}{L}x - 1.02\cosh\frac{4.73}{L}x \right) \tag{8.50}$$

Introducing equation (8.38) into (8.36), multiplying the result by $\phi_1(x)$, integrating over the domain $0 < x < L$

$$Y_1(t)\int_0^L EI\frac{d^4\phi_1(x,t)}{dx^4}\phi_1(x)dx + C\dot{Y}_1(t)\int_0^L \phi_1^2(x)dx + \ddot{Y}_1(t)\int_0^L \rho\phi_1^2(x)dx = \int_0^L \phi_1(x)F_C dx \tag{8.51}$$

Considering the following condition

$$\int_0^L EI\frac{d^4\phi_1(x,t)}{dx^4}\phi_1(x)dx = \omega_1^2 \tag{8.52}$$

Equation of $Y_1(t)$ can be expressed as

$$\ddot{Y}_1(t) + 2\xi_1\omega_1\dot{Y}_1(t) + \omega_1^2 Y_1(t) = P_1 \tag{8.53}$$

$$P_1 = \int_0^L \phi_1(x)\cdot F_C \sin\theta\, \delta(x_c)dx = \phi_1(x)\cdot F_C \sin\theta\Big|_{x=x_c} \tag{8.54}$$

$$\overline{\omega}_1 = \omega_1 \cdot \sqrt{1-\xi^2} \tag{8.55}$$

The solution to $Y_1(t)$ is given by:

$$Y_1(t) = e^{-\xi_1\omega_1 t}\left(B_1(t)\cos\overline{\omega}_1 t + C_1(t)\sin\overline{\omega}_1 t\right) + D_1(t) \tag{8.56}$$

where

$$B_1(t) = \rho\int_0^L v_1(x,0)\cdot\phi_1(x)dx \tag{8.57}$$

$$C_1(t) = \frac{\rho}{\overline{\omega}_1}\int_0^L \left(\dot{v}_1(x,0) + \xi_1\omega_1 v_1(x,0)\right)\dot{v}_1(x,0)\cdot\phi_1(x)dx \tag{8.58}$$

$$D_1(t) = \frac{1}{\overline{\omega}_1}\int_0^t P_1 \cdot e^{-\xi_1\omega_1(t-\tau)}\sin\left[\overline{\omega}_1(t-\tau)\right]d\tau \tag{8.59}$$

The value of damping factor ξ is usually obtained experimentally. If no empirical value exit for a particular ship, measured internal damping values from many ships are

presented in reference (ISSC, 1983). These values indicate that damping factor is practically independent of frequency and a value $\xi = 0.05$ may be used.

Bending moment induced by the transverse hull beam vibration is

$$M(x,t) = EI \cdot \frac{\partial^2 v(x,t)}{\partial^2 x} \tag{8.60}$$

The global elastic bending energy induced by transverse vibration

$$E_{VB}(x,t) = \int_0^L \frac{M^2(x,t)}{2EI} dx = \int_0^L \frac{EI}{2} \cdot \left(\frac{\partial^2 v(x,t)}{\partial x^2} \right)^2 dx \tag{8.61}$$

The kinetic energy of hull beam transverse vibration can be expressed

$$E_{VK}(x,t) = \frac{1}{2} \int_0^L \rho \cdot \left(\frac{\partial v(x,t)}{\partial t} \right)^2 dt \tag{8.62}$$

The total energy caused by transverse vibration is

$$E_V(x,t) = E_{VB} + E_{VK} \tag{8.63}$$

8.3.4 New Simplified Analytical Internal Mechanics Model

Here, a new simplified analytical internal mechanics model is proposed. The idea is that the work of an external force must equal the plastic deformed energy dissipation in the local structure E_{LP}, elastic bending energy and kinetic induced by transverse hull vibration E_V, kinetic energy of struck ship for surge, sway, roll, pitch and yaw motion E_{GK}.

The new simplified analytical internal mechanics model can be expressed as

$$\int_0^{\delta_n} F_C^{New}(\delta) \cdot d\delta = \int_0^{\delta_n} \left(F^{prev}(\delta) + F_{Dyna}(\delta) \right) \cdot d\delta = E_{LP} + E_V + E_{GK} \tag{8.64}$$

8.4 Verification of New Simplified Analytical Internal Mechanics Model

In order to check the accuracy of the present simplified analytical internal mechanics model, the same ship collision case in section 6.4 is used. The relative parameters for this side ship collision case are as following:

Initial velocity of striking ship:	$V_0^a = 16 \quad knot$
Collision location:	$x_C = \frac{L}{2} = 163.5\ m$ (midship)
Collision angle:	$\theta = 90°$
Flexural stiffness of struck ship hull beam:	$EI = 6.3 \times 10^{14} \quad N * m^2$
Damping factor:	$\varsigma = 0.05$
Added mass coefficients:	$\frac{A_{11}^b}{M^b} = 0.05;\quad \frac{A_{22}^b}{M^b} = 0.24;$
	$\frac{A_{55}^b}{I_{yy}^b} = \frac{A_{66}^b}{I_{zz}^b} 0.21$
Spring model parameters for roll motion:	$K_{eq} = 3.66 \times 10^7\ N/m$
	$B_1 = 11.46\ m$

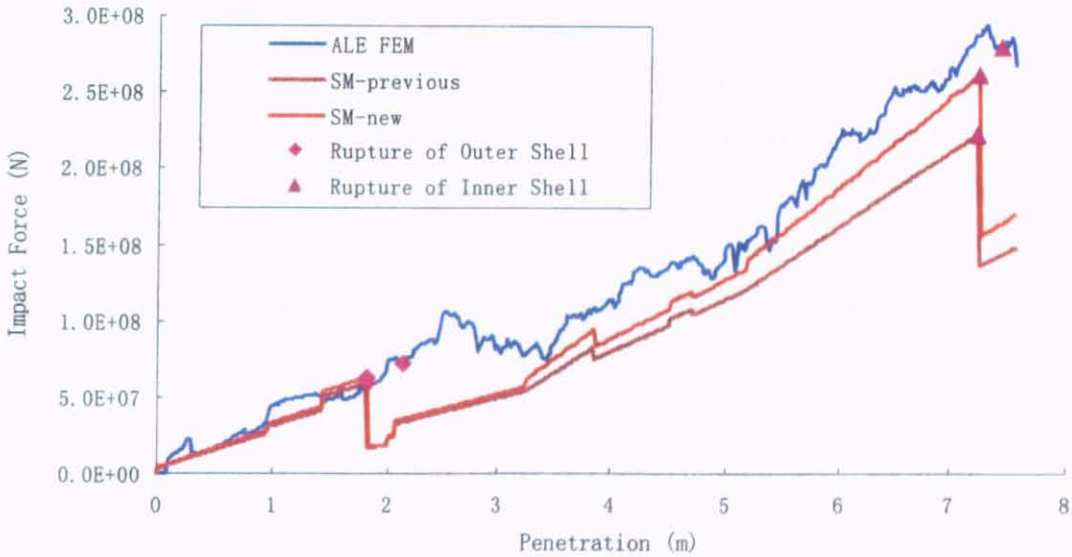

Fig. 8.9 Impact force-penetration curve for different methods

In this collision case, the induced motions of struck ship include sway and roll. Applying the new simplified analytical model, the impact force-penetration curves using previous simplified analytical model, new simplified analytical model and ALE FEM are plotted in Fig. 8.9. At the time of inner shell rupture, the new simplified analytical model can increase 16% impact force compared with the results of previous simplified analytical model.

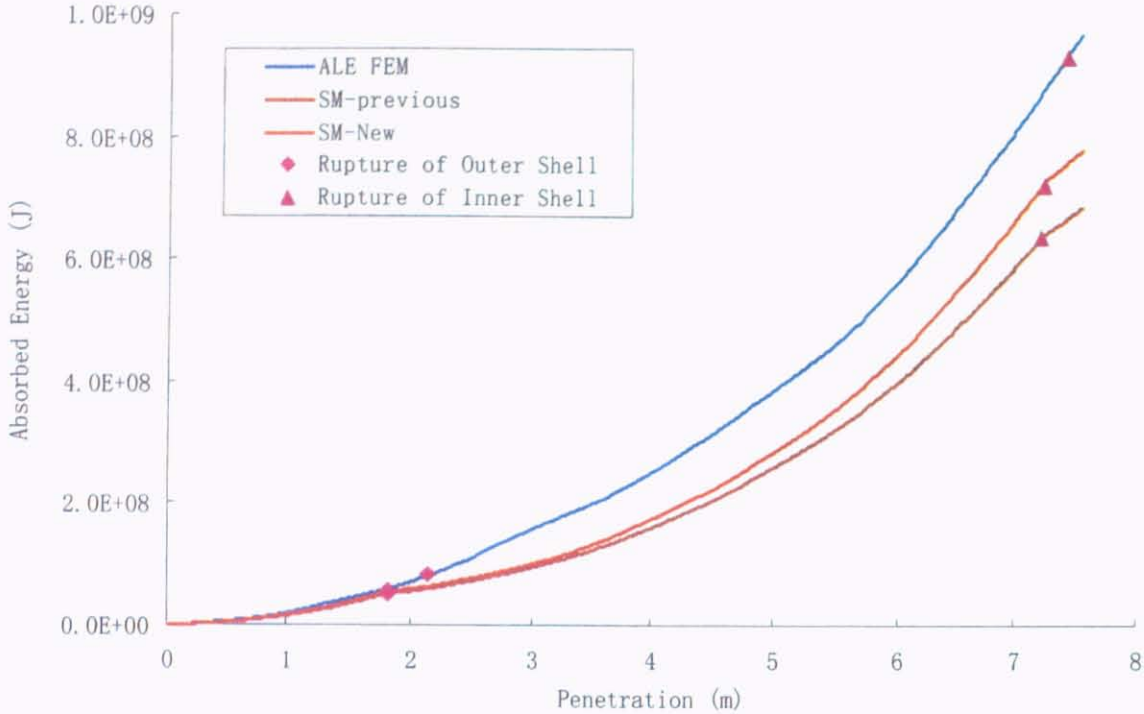

Fig. 8.10 Total absorbed energy-penetration curve for different methods

Fig. 8.10 shows total absorbed energy of struck ship for different methods. In Table 8.2, the penetration depths, impact forces, total absorbed energy at the point of inner shell rupture for previous simplified analytical model, new simplified analytical model and ALE FEM are given. Compared with ALE FEM result, the accuracy of new simplified analytical method is higher than the previous simplified mechanics method.

Table 8.2 Calculation results for struck ship using different methods

	Previous model	Present model	ALE FEM
Time of Inner Shell Rupture(s)	0.924	0.926	0.972
Penetration Depth (m)	7.24	7.26	7.45
Impact Force (MN)	223	262	280
Total absorbed Energy of Struck Ship(MJ)	634	718	926

8.5 Benchmark Studies on New Simplified Analytical Model and Nonlinear FEM for Ship Side Collisions

In new simplified analytical model, three control variables, which are striking velocity (V_a), collision angle (θ) and collision location ($\frac{x}{L}$), can be taken into account. Compared with ALE FE simulation results for a variety of ship side collision scenarios in chapter 7, benchmark studies on present model are performed in this section.

- **Effect of striking velocity**

Using new simplified analytical model, numerical calculations for side collision between 72,000 tonne oil tanker and 293,000 tonne VLCC are performed for the initial striking velocity with 16knot, 14knot and 12knot. The principal dimensions and material properties of the striking/struck ships are the same as those of the model in chapter 5, which are shown in Table 5.1, 5.2.

The impact force-penetration curves for different striking velocities are plotted in Fig. 8.11. Fig. 8.12 shows total absorbed energy-penetration of struck ship for different striking velocities.

In Table 8.3, the penetration depths, impact forces, total absorbed energy at the point of inner shell rupture for different striking velocities are given.

Table 8.3 Calculation results for struck ship for different striking velocities

Striking Velocity (knot)	16		14		12	
	Present model	ALE FEM	Present model	ALE FEM	Present model	ALE FEM
Time of Inner Shell Rupture(s)	0.62	0.58	0.78	0.97	1.09	1.20
Penetration (m)	5.99	5.65	5.97	5.95	6.00	5.84
Impact Force (MN)	215	220	217	232	223	218
Total absorbed Energy (MJ)	486	623	481	643	491	625

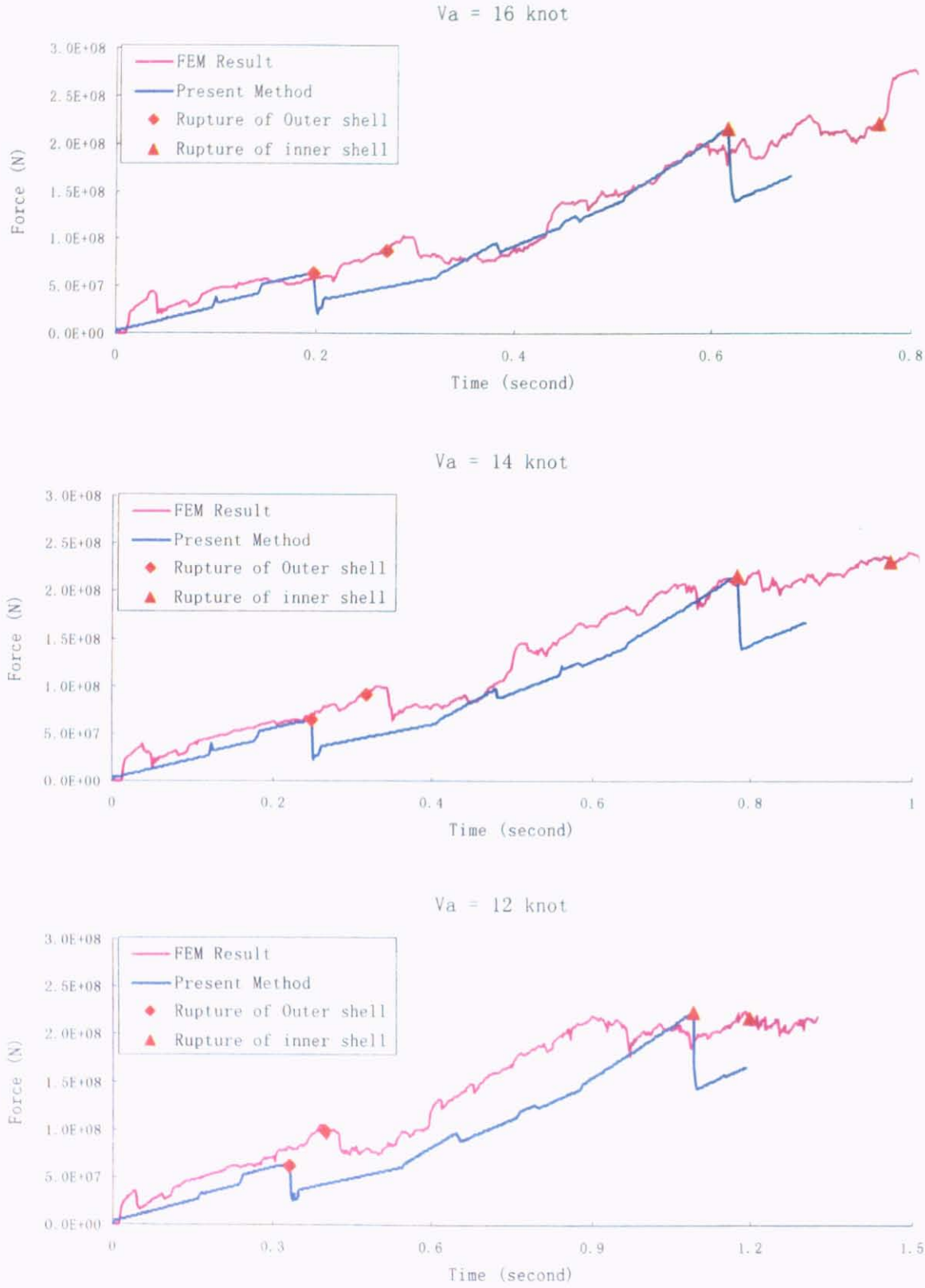

Fig. 8.11 Impact force-penetration curve for different striking velocities

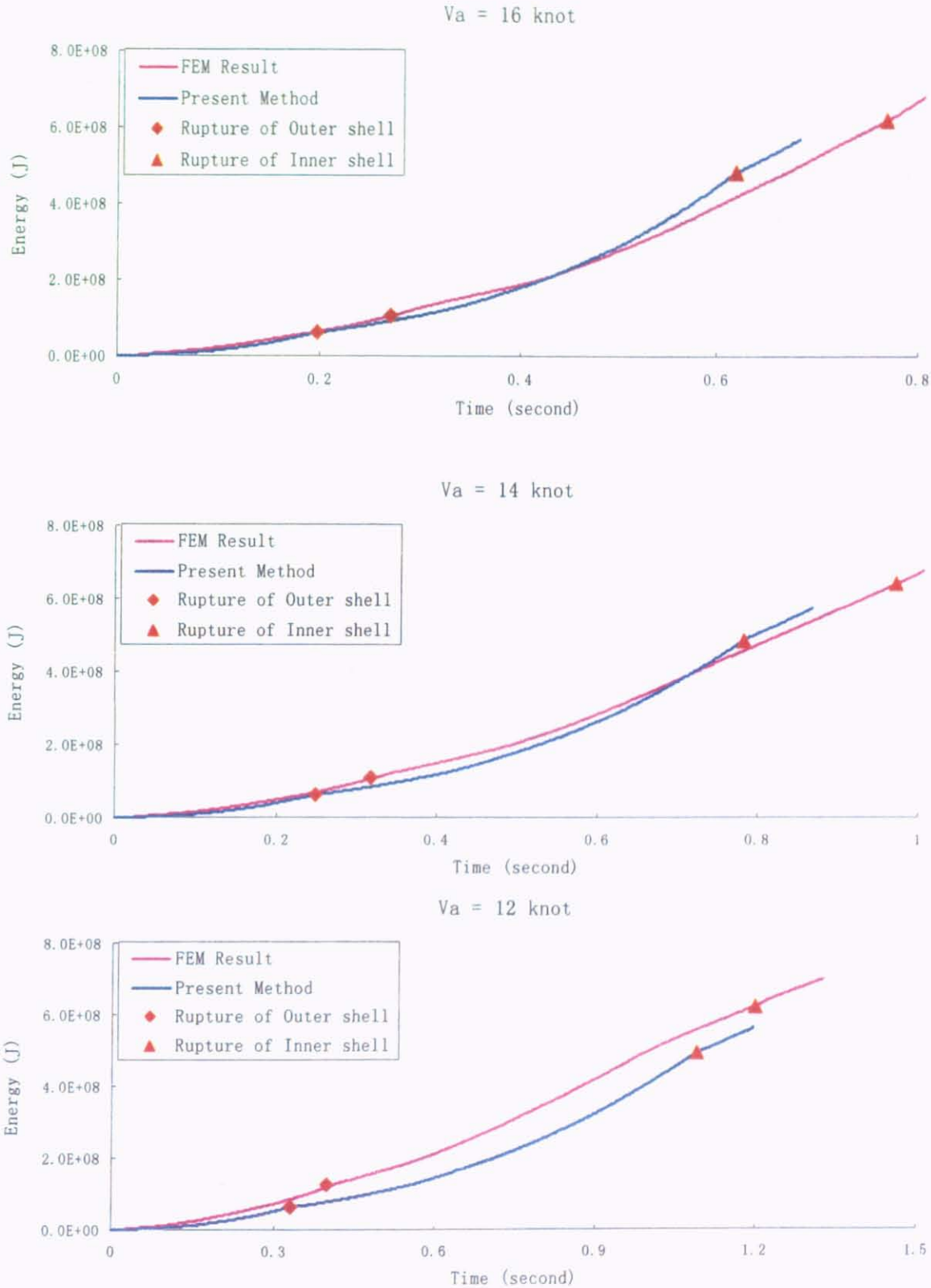

Fig. 8.12 Absorbed energy-penetration curve for different striking velocities

Numerical calculation results of new simplified analytical model show that the impact force and absorbed internal energy is similar at the time of inner shell rupture for various initial striking velocities, which is the same conclusion derived by ALE FEM simulation results. Compared with FEM result, the accuracy of predicted impact force is better than that of absorbed energy.

- **Effect of collision angle**

In new simplified analytical model, we assume that the component of the impact force ($F_C(\theta)$) along the direction of penetration (δ) is same when the collision angle is 90° (as Fig.8.13 shown):

$$F_C(\theta) = \frac{F_C(90^\circ)}{\sin\theta} \tag{8.63}$$

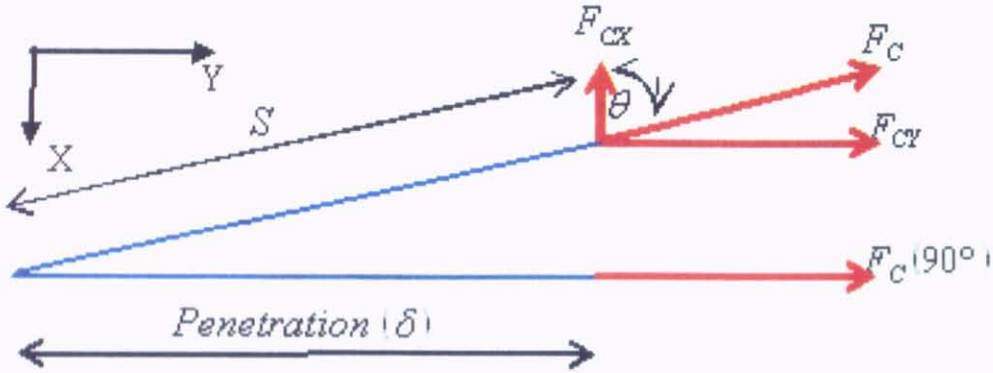

Fig. 8.13 Impact force components for collision angle θ

Using new simplified analytical model, numerical calculations for side collision between 72,000 tonne oil tanker and 293,000 tonne VLCC are performed for the collision angle with 90 degree, 75 degree and 60 degree. The principal dimensions and material properties of the striking/struck ships are the same as those of the model in chapter 5, which are shown in Table 5.1, 5.2.

The impact force-penetration curves for different collision angles are plotted in Fig. 8.14. Fig. 8.15 shows total absorbed energy-energy of struck ship for different collision angles. In Table 8.4, the penetration depths, impact forces, total absorbed energy at the point of inner shell rupture for different collision angles are given.

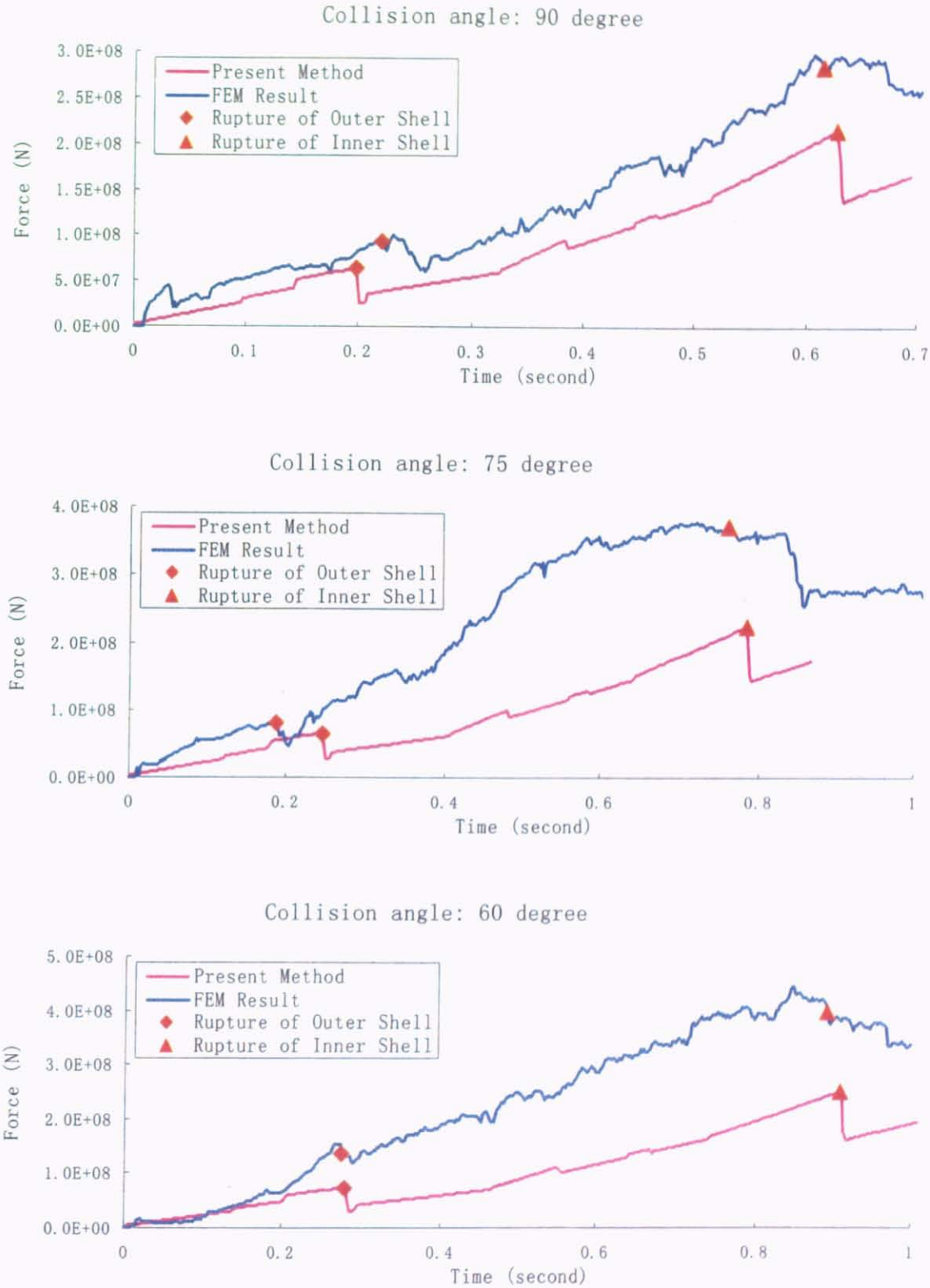

Fig. 8.14 Impact force-penetration curve for different collision angles

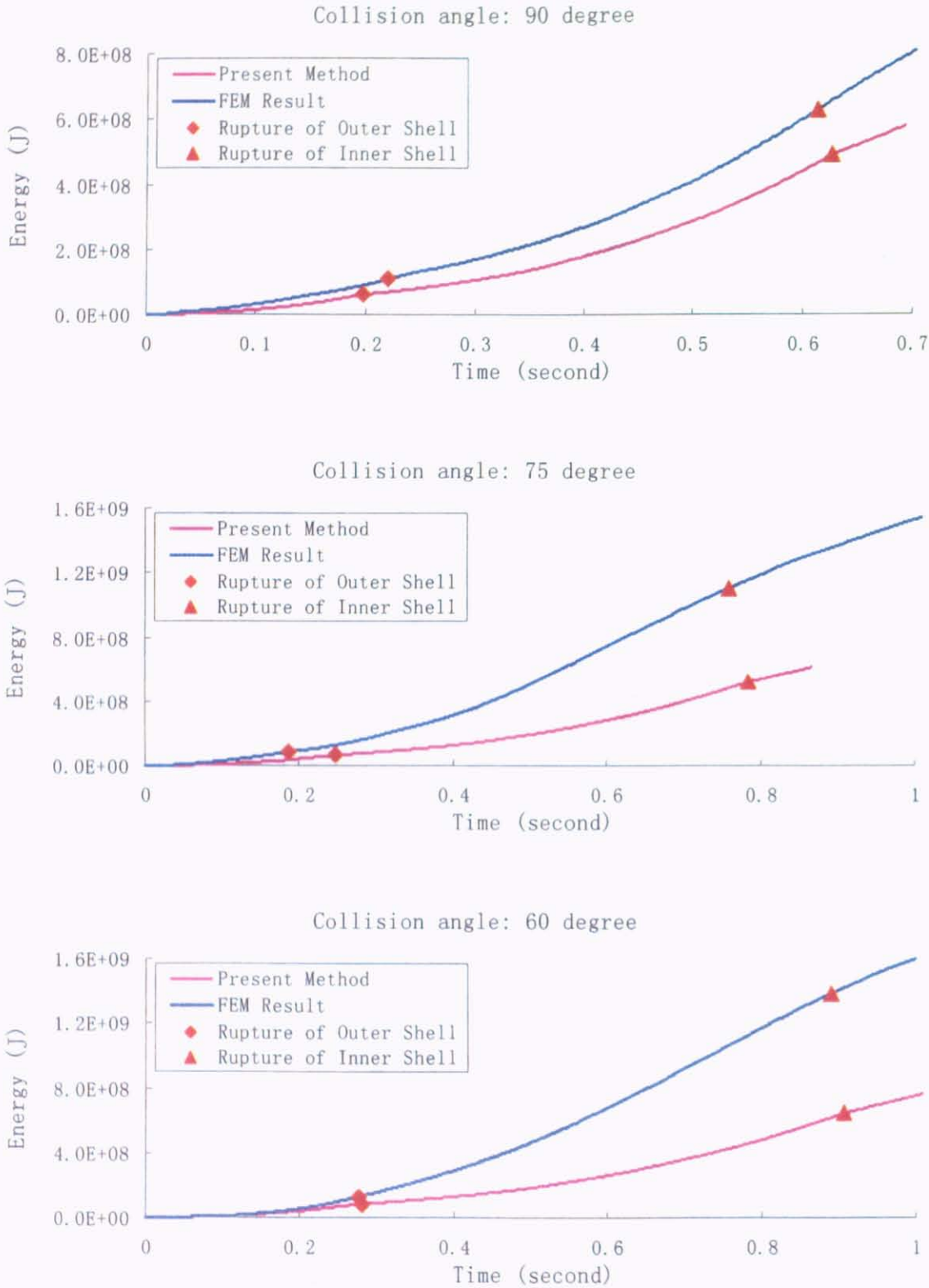

Fig. 8.15 Absorbed energy-penetration curve for different collision angles

Table 8.4 Calculation results for struck ship for different collision angles

Collision angle (degree)	90		75		60	
	Present model	ALE FEM	Present model	ALE FEM	Present model	ALE FEM
Time of Inner Shell Rupture(s)	0.63	0.61	0.78	0.76	0.91	0.89
Penetration (m)	5.99	5.83	6.00	7.54	6.01	7.04
Impact Force (MN)	217	287	224	372	252	399
Total absorbed Energy (MJ)	487	646	522	1107	650	1387

From the comparison in Table 8.4, it is seen that the new simplified analytical method can consider the effect of collision angle on impact force and absorbed energy reasonable. Smaller collision angle leads to larger resistance of side structures at the time of inner shell rupture. To impact force and total absorbed energy at the point of inner shell rupture, the agreement for collision angle 90 degree is excellent. The difference for collision angle 60 is relatively large. Similar to the conclusion derived by ALE FEM simulation results, the perpendicular collision ($90°$) causes the maximum impact force and absorbed energy of side structures at the same collision time.

- **Effect of collision location**

Using new simplified analytical model, numerical calculations for side collision between 350,000 tonne VLCC and 293,000 tonne VLCC are performed for the collision location ($\frac{x}{L}$) with 0.2, 0.5 and 0.65. The principal dimensions and material properties of the striking/struck ships are the same as those of the model in chapter 6.

The impact force-penetration curves for different collision locations are plotted in Fig. 8.16. Fig. 8.17 shows total absorbed energy-energy of struck ship for different collision location. In Table 8.5, the penetration depths, impact forces, total absorbed energy at the point of inner shell rupture for different collision locations are given.

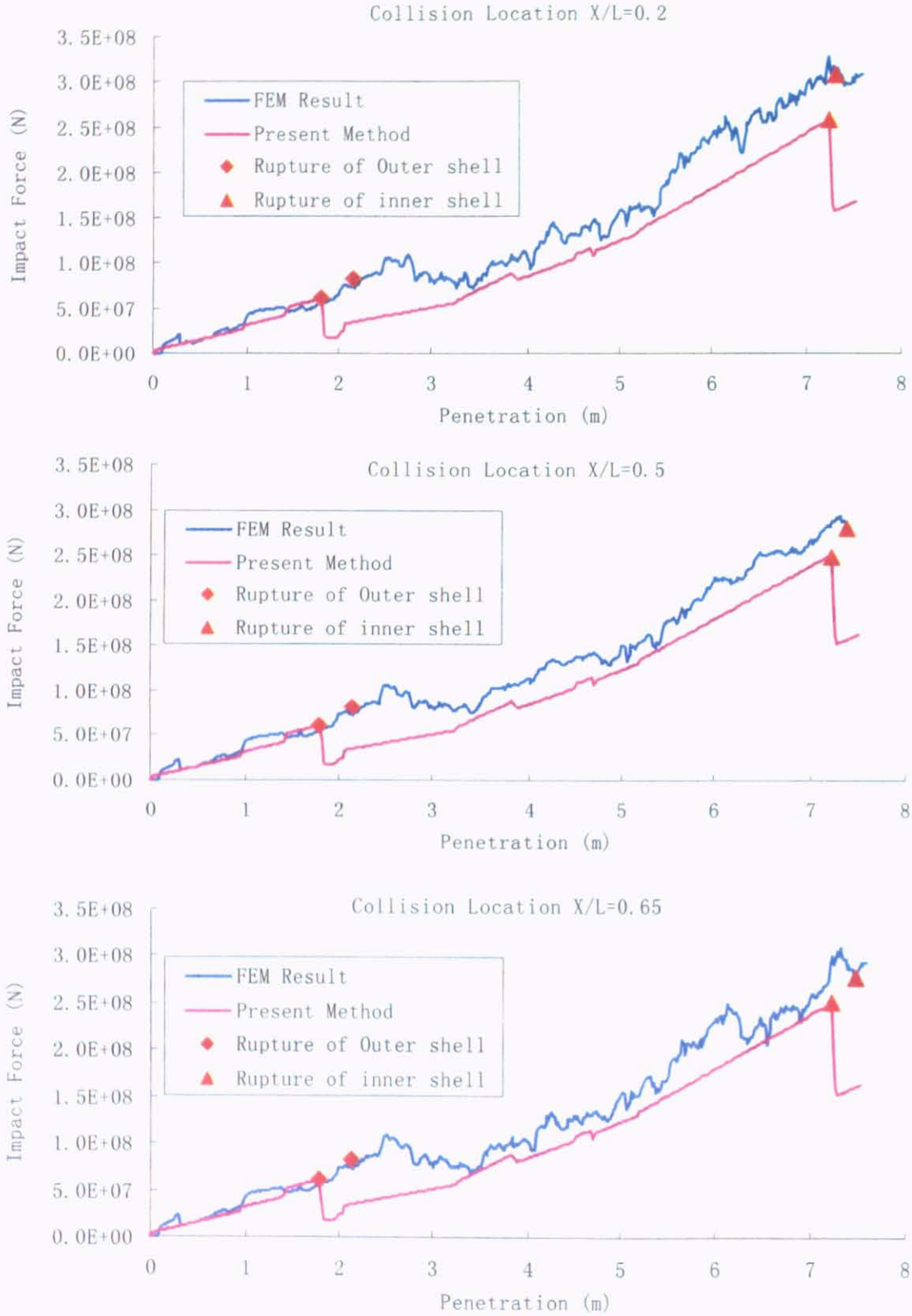

Fig. 8.16 Impact force-penetration curve for different collision locations

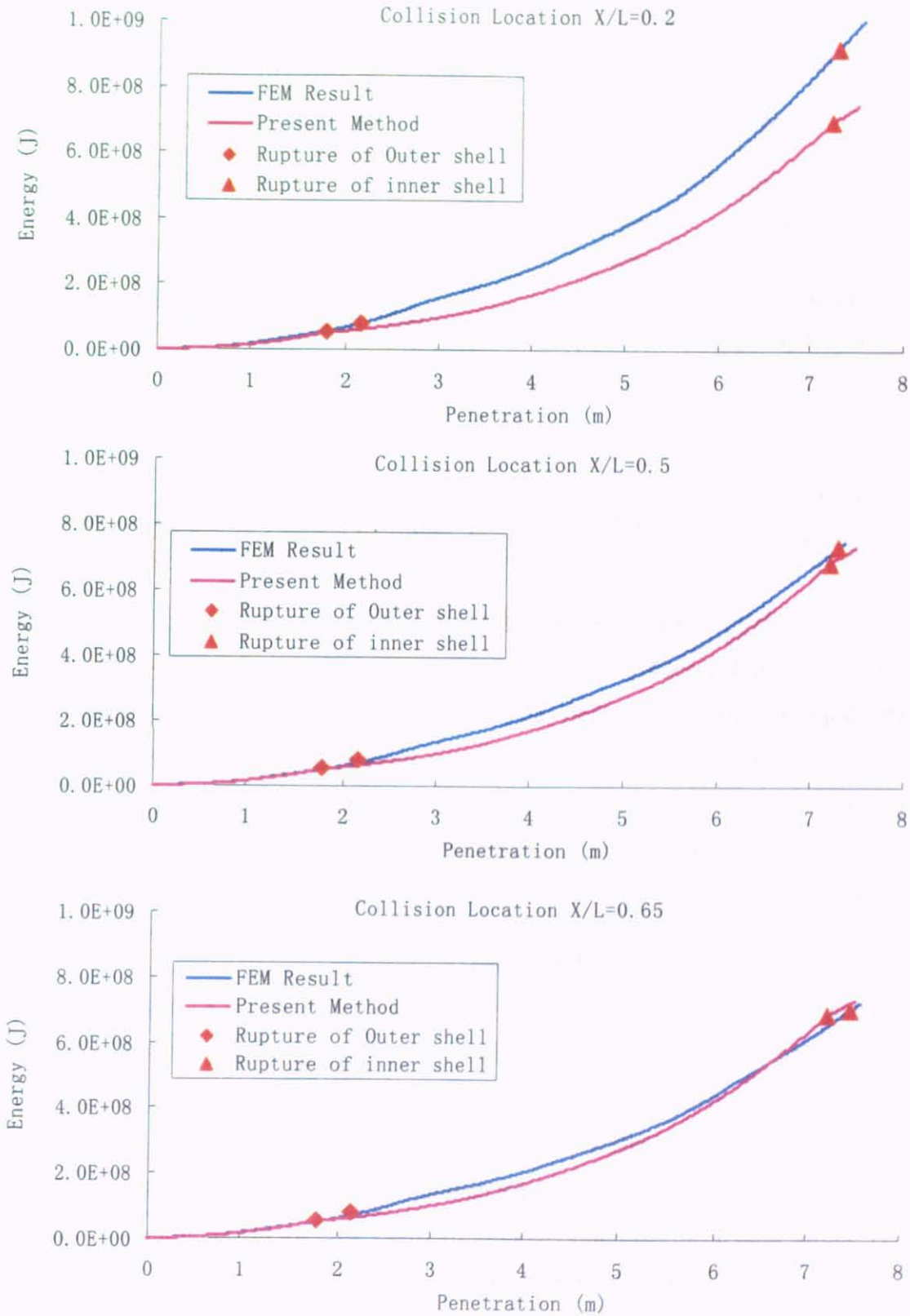

Fig. 8.17 Absorbed energy-penetration curve for different collision locations

Table 8.5 Calculation results for struck ship for different collision locations

Collision location (X/L)	0.2		0.5		0.65	
	Present model	ALE FEM	Present model	ALE FEM	Present model	ALE FEM
Time of Inner Shell Rupture(s)	1.062	0.904	1.062	0.892	1.062	0.882
Penetration (m)	7.231	7.299	7.233	7.327	7.232	7.480
Impact Force (MN)	258.6	308.2	248.5	294.6	251.0	277.34
Total absorbed Energy (MJ)	697.0	921.0	683.5	736.3	686.9	705.3

In new simplified analytical model, different collision location cause different extent yaw motion of struck ship. From the comparison in Fig. 8.17 and Table 8.5, it is seen that the new simplified analytical method can consider the effect of collision location on impact force and absorbed energy reasonable. To impact force at the point of inner shell rupture, the agreement for collision location 0.65 is excellent. The difference for collision location 0.2 is relatively large. The agreement for impact force at rupture of outer and inner shell for different collision location is better than that of total absorbed energy.

- **Effect of different striking ships**

Using new simplified analytical model, numerical calculations for different striking ship are performed for 72,000 tonne oil tanker, 350,000 tonne VLCC oil tanker for laden condition and ballast condition. The principal dimensions and material properties of the striking/struck ships are the same as those of the model in chapter 5 and 6.

The impact force-penetration curves for different striking ships are plotted in Fig. 8.18. Fig. 8.19 shows total absorbed energy-energy of struck ship for different striking ships. In Table 8.6, the penetration depths, impact forces, total absorbed energy at the point of inner shell rupture for different ships are given.

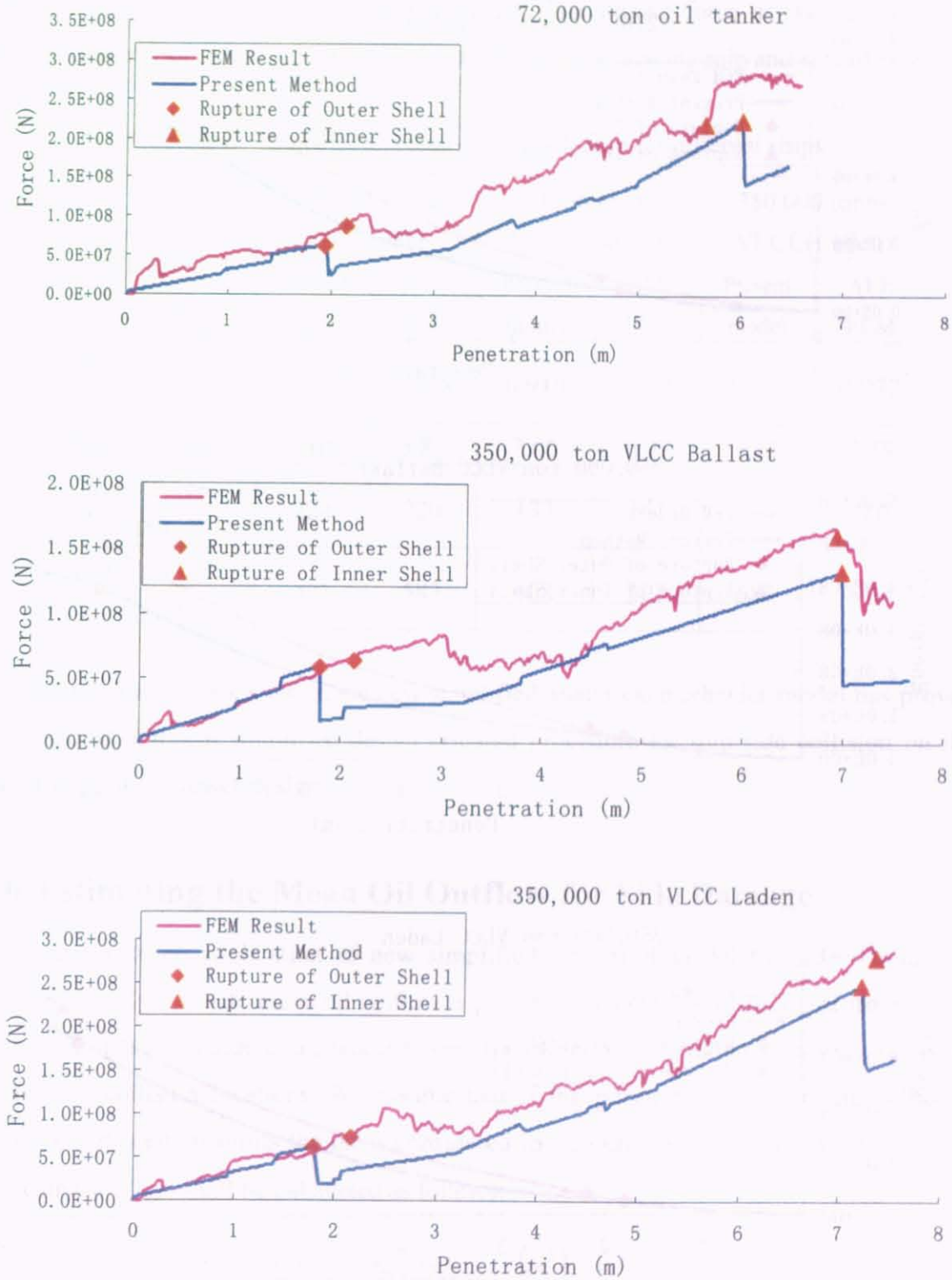

Fig. 8.18 Impact force-penetration curve for different ships

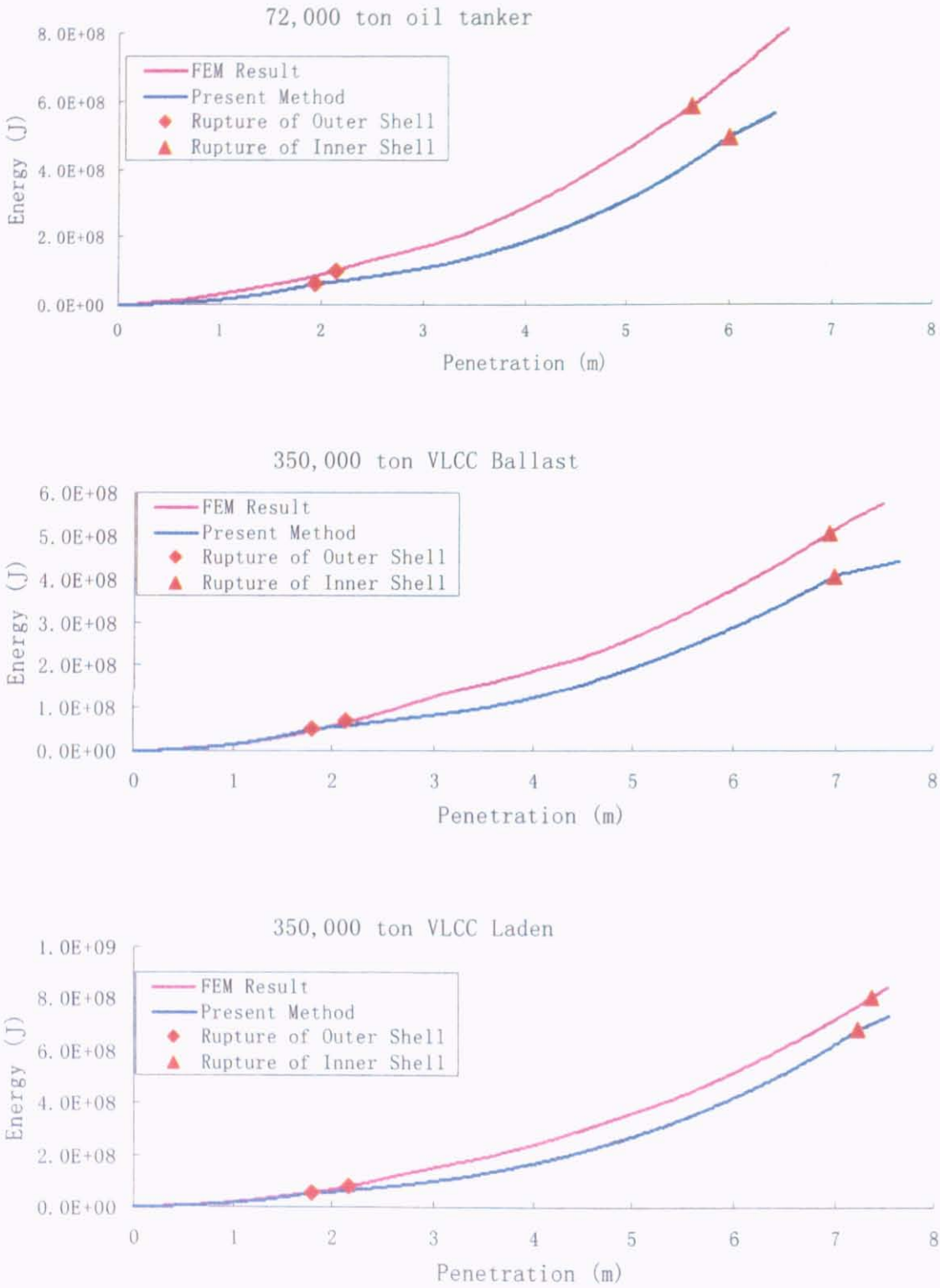

Fig. 8.19 Absorbed energy-penetration curve for different ships

From the comparison in Table 8.6, it is seen that the general agreement between the present method and FEM results is reasonable. The impact force as well as the total absorbed energy of side structures varied with the mass of striking ship and size of bow.

Table 8.6 Calculation results for struck ship for different ships

Ship Type	72,000 tonne Oil Tanker		350,000 tonne VLCC(Ballast)		350,000 tonne VLCC(Laden)	
	Present model	ALE FEM	Present model	ALE FEM	Present model	ALE FEM
Time of Inner Shell Rupture(s)	0.798	0.768	0.910	0.916	1.062	0.972
Penetration (m)	6.01	5.83	7.00	6.95	7.23	7.38
Impact Force (MN)	224	220	133	161	248	280
Total absorbed Energy (MJ)	493	583	408	507	683	810

Through benchmark studies, the new simplified analytical mechanics model has proved to a rational practical simplified design oriented procedure for ship side collision on the initial stage of oil tanker design

8.6 Estimating the Mean Oil Outflow for Side Damage

In this section, application of new simplified analytical model for side damage to probabilistically estimate mean oil outflow is presented. Here the probability of penetrating cargo tank in case of side collisions considers the effect of the striking velocities, collision angles and collision locations. We assume that if the penetration between the colliding ships exceeds certain limits the oil is considered to be outflow. The mean oil outflow for side damage O_{MS} shall be calculated as follows:

$$O_{MS} = \sum P_S\left(V_a, \theta, \frac{x}{L}\right) \cdot O_S \qquad (m^3) \tag{8.64}$$

Where

P_S probability of penetrating cargo tank from side damage considering the effect of striking velocity (V_a), collision angle (θ) and location ($\frac{x}{L}$).

O_S oil outflow from side damage to cargo tank, which is assumed equal to the total volume in cargo tank, in m^3.

Based on the ship collision database of Japan, Endo et al (2005) assume that probability density function (PDF) of the striking velocities is uniform distribution. For VLCC of striking ship, the range of striking velocities is from 0 to 16 knot with 1 knot incremental (as Fig.8.17 shown). Similar to the striking velocity case, the PDF of collision angles is assumed the uniform distribution (from 0 degree to 180 degree with 5 degree incremental, as Fig.8.18 shown). The PDF of collision location specifies a uniform constant value over the entire length of the struck ship (as Fig.8.19 shown).

Based on the Sandia National Laboratory Report(1998) and USCG ship casualty data(1991), Brown(2002) uses a Normal distribution ($\mu = 90$ degrees, $\sigma = 28.97$ degrees) to describe the PDF of collision angle. The PDF of striking velocity is plotted in Fig.8.18.

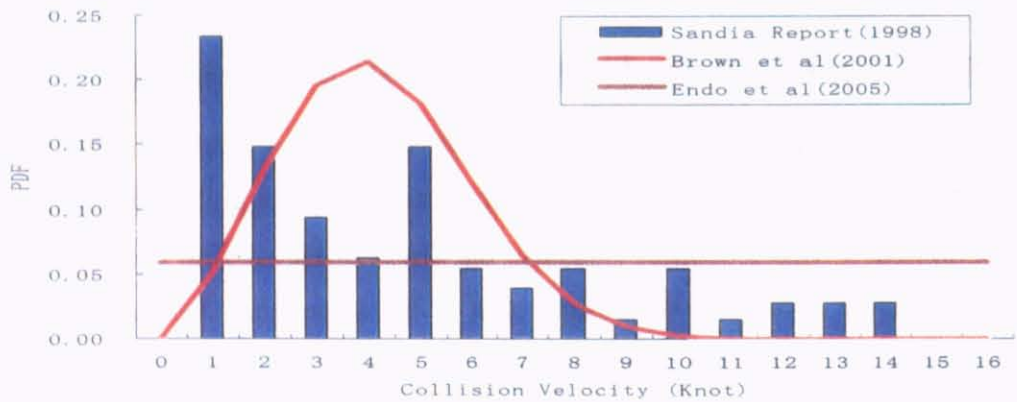

Fig. 8.20 Striking ship velocity PDF

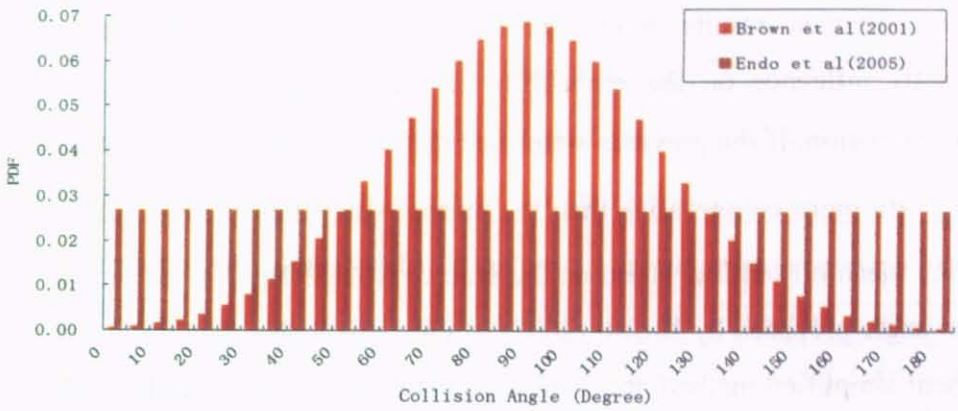

Fig. 8.21 Collision angle PDF

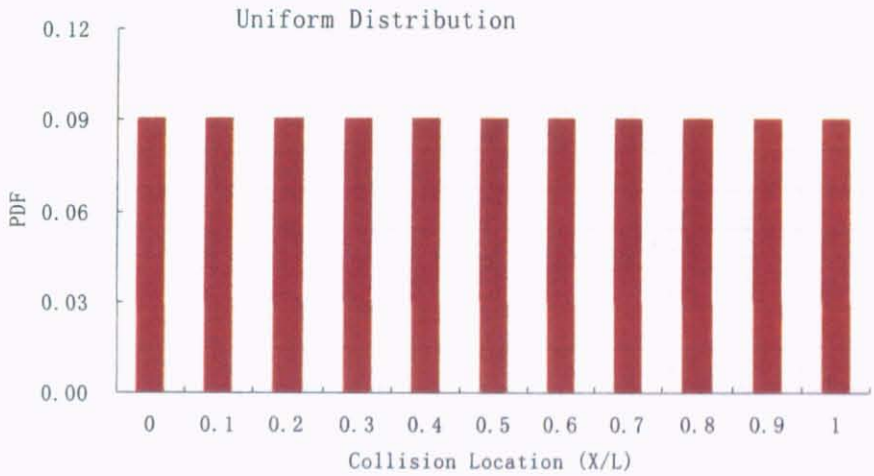

Fig. 8.22 Collision location PDF

Application of previous simplified method and present simplified method, a series of calculations are performed for 293,000 tonne VLCC struck by 350,000 tonne VLCC. Table 8.6 and 8.7 provide the map of penetrating cargo tank for different collision angles and striking velocities, respectively.

The probability of penetrating cargo tank from side damage (P_S) and the mean oil outflow (O_{MS}) are estimated by using previous simplified method, present method. Based on the revised draft of MARPOL 73/78 Annex I (IMO BLG 2003), a probabilistic method estimating oil outflow from a struck tanker is also performed. The results are presented in table 8.8 comparing to each other.

The estimation results show that PDF of striking velocity and collision angle significantly influence on the probability of penetrating cargo tank and the mean oil outflow estimation. If the previous simplified method is used, the estimating results of P_S and O_{MS} are more conservative than the present simplified method. Compared with the estimation mean oil outflow based on the draft of MARPOL, PDF of striking velocity and collision angle proposed by Brown (2002) is more reasonable than Endo(2005). Combined the present simplified method and PDF of collision angles and striking velocity proposed by Brown (2002), a good estimating result of P_S and O_{MS} can be obtained.

Table 8.7 Map of penetrating cargo tank using present method

$V_a = 16\ knot$		Collision Angle (degree)												
		25	30	35	40	45	50-60	65-110	115-125	130	135-140	145	150	155
Collision Location(X/L)	0						O	O						
	0.1			O	O	O	O	O	O	O				
	0.2			O	O	O	O	O	O	O	O			
	0.3		O	O	O	O	O	O	O	O	O	O	O	
	0.4		O	O	O	O	O	O	O	O	O	O	O	O
	0.5	O	O	O	O	O	O	O	O	O	O	O	O	O
	0.6		O	O	O	O	O	O	O	O	O	O	O	O
	0.7			O	O	O	O	O	O	O	O	O	O	
	0.8					O	O	O	O	O	O	O	O	
	0.9						O	O	O	O	O	O		
	1							O	O					

$V_a = 15\ knot$		Collision Angle (degree)													
		25	30	35	40	45	50-55	60	65-110	115-125	130	135-140	145	150	155
Collision Location(X/L)	0							O	O						
	0.1				O	O	O	O	O	O	O				
	0.2			O	O	O	O	O	O	O	O	O			
	0.3			O	O	O	O	O	O	O	O	O	O		
	0.4		O	O	O	O	O	O	O	O	O	O	O	O	
	0.5	O	O	O	O	O	O	O	O	O	O	O	O	O	O
	0.6		O	O	O	O	O	O	O	O	O	O	O	O	
	0.7			O	O	O	O	O	O	O	O	O	O		
	0.8					O	O	O	O	O	O	O	O		
	0.9						O	O	O	O	O	O			
	1								O	O					

$V_a = 14\ knot$		Collision Angle (degree)										
		30	35-40	45	50-55	60	65-110	115-125	130	135-140	145	150
Collision Location(X/L)	0					O	O					
	0.1		O	O	O	O	O	O	O			
	0.2		O	O	O	O	O	O	O	O		
	0.3		O	O	O	O	O	O	O	O	O	
	0.4	O	O	O	O	O	O	O	O	O	O	O
	0.5	O	O	O	O	O	O	O	O	O	O	O
	0.6	O	O	O	O	O	O	O	O	O	O	O
	0.7		O	O	O	O	O	O	O	O	O	O
	0.8			O	O	O	O	O	O	O	O	
	0.9				O	O	O	O	O	O	O	
	1						O	O				

"O" means the penetration of cargo tank occurred

$V_a = 13\ knot$		Collision Angle (degree)										
		30	35-40	45-55	60	65-75	80-100	105-115	120	125-135	140-145	150
Collision Location(X/L)	0					○	○					
	0.1			○	○	○	○	○	○			
	0.2		○	○	○	○	○	○	○	○		
	0.3	○	○	○	○	○	○	○	○	○	○	
	0.4	○	○	○	○	○	○	○	○	○	○	○
	0.5	○	○	○	○	○	○	○	○	○	○	○
	0.6	○	○	○	○	○	○	○	○	○	○	○
	0.7		○	○	○	○	○	○	○	○	○	○
	0.8			○	○	○	○	○	○	○	○	
	0.9				○	○	○	○	○	○		
	1						○	○				

$V_a = 12\ knot$		Collision Angle (degree)										
		35	40	45	50-55	60-75	80-105	110-115	120	125-135	140	145
Collision Location(X/L)	0					○	○					
	0.1				○	○	○	○	○			
	0.2		○	○	○	○	○	○	○	○		
	0.3	○	○	○	○	○	○	○	○	○	○	
	0.4	○	○	○	○	○	○	○	○	○	○	○
	0.5	○	○	○	○	○	○	○	○	○	○	○
	0.6	○	○	○	○	○	○	○	○	○	○	○
	0.7		○	○	○	○	○	○	○	○	○	○
	0.8			○	○	○	○	○	○	○	○	
	0.9					○	○	○	○	○		
	1						○	○				

$V_a = 11\ knot$		Collision Angle (degree)										
		35	40	45-50	55	60-70	75-80	85-95	100-105	110-120	125-135	140
Collision Location(X/L)	0						○	○				
	0.1				○	○	○	○	○	○		
	0.2		○	○	○	○	○	○	○	○	○	
	0.3	○	○	○	○	○	○	○	○	○	○	
	0.4	○	○	○	○	○	○	○	○	○	○	○
	0.5	○	○	○	○	○	○	○	○	○	○	○
	0.6	○	○	○	○	○	○	○	○	○	○	○
	0.7		○	○	○	○	○	○	○	○	○	○
	0.8			○	○	○	○	○	○	○	○	
	0.9					○	○	○	○	○	○	
	1							○	○			

"○" means the penetration of cargo tank occurred

$V_a = 10\ knot$	Collision Angle (degree)											
Collision Location(X/L)	40	45-50	55-60	65-70	75-80	85	90-105	110-115	120-125	130	135	140
0							O					
0.1				O	O	O	O					
0.2		O	O	O	O	O	O	O	O			
0.3	O	O	O	O	O	O	O	O	O	O	O	
0.4	O	O	O	O	O	O	O	O	O	O	O	O
0.5	O	O	O	O	O	O	O	O	O	O	O	O
0.6	O	O	O	O	O	O	O	O	O	O	O	O
0.7		O	O	O	O	O	O	O	O	O	O	O
0.8			O	O	O	O	O	O	O	O		
0.9					O	O	O	O				
1						O	O					

$V_a = 9\ knot$	Collision Angle (degree)									
Collision Location(X/L)	45	50	55	60-70	75-85	90	95-105	110-120	125-130	135
0										
0.1					O	O				
0.2			O	O	O	O	O	O		
0.3	O	O	O	O	O	O	O	O	O	
0.4	O	O	O	O	O	O	O	O	O	O
0.5	O	O	O	O	O	O	O	O	O	O
0.6	O	O	O	O	O	O	O	O	O	O
0.7		O	O	O	O	O	O	O	O	O
0.8				O	O	O	O	O	O	
0.9						O	O			
1										

$V_a = 8\ knot$	Collision Angle (degree)												
Collision Location(X/L)	55	60	65-70	75	80	85	90	95	100	105	110-115	120	125
0													
0.1					O	O	O						
0.2				O	O	O	O	O					
0.3			O	O	O	O	O	O	O	O	O		
0.4		O	O	O	O	O	O	O	O	O	O	O	
0.5	O	O	O	O	O	O	O	O	O	O	O	O	O
0.6		O	O	O	O	O	O	O	O	O	O	O	
0.7		O	O	O	O	O	O	O	O	O	O		
0.8						O	O	O	O	O			
0.9							O	O	O				
1													

"O" means the penetration of cargo tank occurred

$V_a = 7\ knot$		Collision Angle (degree)								
		70	75	80	85	90	95	100	105	110
Collision Location(X/L)	0									
	0.1			○	○	○				
	0.2		○	○	○	○	○			
	0.3	○	○	○	○	○	○	○		
	0.4	○	○	○	○	○	○	○	○	
	0.5	○	○	○	○	○	○	○	○	○
	0.6		○	○	○	○	○	○	○	○
	0.7			○	○	○	○	○	○	
	0.8				○	○	○	○	○	
	0.9				○	○	○			
	1									

$V_a = 6\ knot$		Collision Angle (degree)				
		80	85	90	95	100
Collision Location(X/L)	0.2					
	0.3		○			
	0.4		○	○		
	0.5		○	○	○	
	0.6			○	○	
	0.7				○	
	0.8					
	0.9					
	1					

Table 8.8 Map of penetrating cargo tank using previous method

$V_a = 16\ knot$		Collision Angle (degree)													
		25	30	35	40	45	50-60	65-110	115-125	130	135-140	145	150	155	160
Collision Location(X/L)	0						○	○							
	0.1			○	○	○	○	○	○	○					
	0.2			○	○	○	○	○	○	○	○				
	0.3		○	○	○	○	○	○	○	○	○	○	○		
	0.4		○	○	○	○	○	○	○	○	○	○	○	○	
	0.5	○	○	○	○	○	○	○	○	○	○	○	○	○	○
	0.6		○	○	○	○	○	○	○	○	○	○	○	○	
	0.7			○	○	○	○	○	○	○	○	○	○	○	
	0.8					○	○	○	○	○	○	○	○		
	0.9						○	○	○	○	○	○			
	1							○	○						

"○" means the penetration of cargo tank occurred

$V_a = 15\ knot$		Collision Angle (degree)													
		25	30	35-40	45	50-55	60	65-110	115-125	130	135-140	145	150	155	160
Collision Location(X/L)	0						○	○							
	0.1			○	○	○	○	○	○	○					
	0.2			○	○	○	○	○	○	○	○				
	0.3		○	○	○	○	○	○	○	○	○	○	○		
	0.4		○	○	○	○	○	○	○	○	○	○	○	○	
	0.5	○	○	○	○	○	○	○	○	○	○	○	○	○	○
	0.6		○	○	○	○	○	○	○	○	○	○	○	○	
	0.7			○	○	○	○	○	○	○	○	○	○	○	
	0.8				○	○	○	○	○	○	○	○	○		
	0.9					○	○	○	○	○	○	○			
	1							○	○						

$V_a = 14\ knot$		Collision Angle (degree)													
		25	30	35-40	45	50-55	60	65-110	115-125	130	135-140	145	150	155	160
Collision Location(X/L)	0						○	○							
	0.1			○	○	○	○	○	○	○					
	0.2			○	○	○	○	○	○	○	○				
	0.3		○	○	○	○	○	○	○	○	○	○	○		
	0.4		○	○	○	○	○	○	○	○	○	○	○		
	0.5	○	○	○	○	○	○	○	○	○	○	○	○	○	○
	0.6		○	○	○	○	○	○	○	○	○	○	○	○	
	0.7			○	○	○	○	○	○	○	○	○	○	○	
	0.8				○	○	○	○	○	○	○	○	○		
	0.9					○	○	○	○	○	○	○			
	1							○	○						

$V_a = 13\ knot$		Collision Angle (degree)										
		30	35-40	45-55	60	65-75	80-100	105-115	120	125-135	140-145	150
Collision Location(X/L)	0					○	○					
	0.1			○	○	○	○	○	○			
	0.2		○	○	○	○	○	○	○	○		
	0.3	○	○	○	○	○	○	○	○	○	○	
	0.4	○	○	○	○	○	○	○	○	○	○	○
	0.5	○	○	○	○	○	○	○	○	○	○	○
	0.6	○	○	○	○	○	○	○	○	○	○	○
	0.7		○	○	○	○	○	○	○	○	○	○
	0.8			○	○	○	○	○	○	○	○	
	0.9				○	○	○	○	○	○		
	1						○	○				

"○" means the penetration of cargo tank occurred

$V_a = 12\ knot$		Collision Angle (degree)													
		30	35	40-45	50	55	60-70	75-105	110	115-120	125-130	135	140	145	150
Collision Location(X/L)	0						O	O							
	0.1				O	O	O	O	O	O					
	0.2		O	O	O	O	O	O	O	O	O	O			
	0.3	O	O	O	O	O	O	O	O	O	O	O	O		
	0.4	O	O	O	O	O	O	O	O	O	O	O	O	O	O
	0.5	O	O	O	O	O	O	O	O	O	O	O	O	O	O
	0.6	O	O	O	O	O	O	O	O	O	O	O	O	O	O
	0.7		O	O	O	O	O	O	O	O	O	O	O	O	
	0.8			O	O	O	O	O	O	O	O	O	O		
	0.9					O	O	O	O	O	O				
	1							O	O						

$V_a = 11\ knot$		Collision Angle (degree)												
		30-35	40	45-50	55	60-70	75-80	85-95	100-105	110-120	125-135	140	145	150
Collision Location(X/L)	0						O	O						
	0.1				O	O	O	O	O	O				
	0.2		O	O	O	O	O	O	O	O	O			
	0.3	O	O	O	O	O	O	O	O	O	O	O		
	0.4	O	O	O	O	O	O	O	O	O	O	O	O	O
	0.5	O	O	O	O	O	O	O	O	O	O	O	O	O
	0.6	O	O	O	O	O	O	O	O	O	O	O	O	O
	0.7		O	O	O	O	O	O	O	O	O	O	O	O
	0.8			O	O	O	O	O	O	O	O	O	O	
	0.9					O	O	O	O	O	O			
	1							O	O					

$V_a = 10\ knot$		Collision Angle (degree)													
		35	40	45-50	55-60	65-70	75-80	85	90-105	110-115	120-125	130	135	140	145
Collision Location(X/L)	0								O						
	0.1					O	O	O	O						
	0.2			O	O	O	O	O	O	O	O				
	0.3		O	O	O	O	O	O	O	O	O	O	O		
	0.4	O	O	O	O	O	O	O	O	O	O	O	O	O	
	0.5	O	O	O	O	O	O	O	O	O	O	O	O	O	O
	0.6		O	O	O	O	O	O	O	O	O	O	O	O	O
	0.7			O	O	O	O	O	O	O	O	O	O	O	
	0.8				O	O	O	O	O	O	O	O			
	0.9						O	O	O	O					
	1							O	O						

"O" means the penetration of cargo tank occurred

$V_a = 9\ knot$		Collision Angle (degree)											
		40	45	50	55	60-70	75-85	90	95-105	110-120	125-130	135	140
Collision Location(X/L)	0												
	0.1						○	○					
	0.2				○	○	○	○	○	○			
	0.3		○	○	○	○	○	○	○	○	○		
	0.4	○	○	○	○	○	○	○	○	○	○	○	
	0.5	○	○	○	○	○	○	○	○	○	○	○	○
	0.6		○	○	○	○	○	○	○	○	○	○	○
	0.7			○	○	○	○	○	○	○	○	○	
	0.8					○	○	○	○	○	○		
	0.9							○	○				
	1												

$V_a = 8\ knot$		Collision Angle (degree)													
		45	50-55	60-70	75	80	85	90	95	100	105	110-120	125	130	135
Collision Location(X/L)	0														
	0.1					○	○	○							
	0.2				○	○	○	○	○						
	0.3		○	○	○	○	○	○	○	○	○	○			
	0.4	○	○	○	○	○	○	○	○	○	○	○	○	○	
	0.5	○	○	○	○	○	○	○	○	○	○	○	○	○	○
	0.6		○	○	○	○	○	○	○	○	○	○	○	○	○
	0.7			○	○	○	○	○	○	○	○	○	○		
	0.8						○	○	○	○	○				
	0.9							○	○	○					
	1														

$V_a = 7\ knot$		Collision Angle (degree)												
		55	60	65	70	75	80	85-90	95	100	105	110	115-120	125
Collision Location(X/L)	0													
	0.1						○	○						
	0.2					○	○	○	○	○				
	0.3			○	○	○	○	○	○	○	○			
	0.4	○	○	○	○	○	○	○	○	○	○	○	○	
	0.5	○	○	○	○	○	○	○	○	○	○	○	○	○
	0.6		○	○	○	○	○	○	○	○	○	○	○	○
	0.7				○	○	○	○	○	○	○	○		
	0.8						○	○	○	○	○			
	0.9							○	○	○				
	1													

"○" means the penetration of cargo tank occurred

$V_a = 6\ knot$		Collision Angle (degree)								
		70	75	80	85	90	95	100	105	110
Collision Location(X/L)	0									
	0.1					O				
	0.2				O	O	O			
	0.3		O	O	O	O	O	O		
	0.4	O	O	O	O	O	O	O	O	
	0.5	O	O	O	O	O	O	O	O	O
	0.6		O	O	O	O	O	O	O	O
	0.7			O	O	O	O	O	O	
	0.8					O	O	O		
	0.9						O			
	1									

"O" means the penetration of cargo tank occurred

Table 8.9 Estimated mean oil outflow

	Endo's Assumption		Brown's Assumption		IMO BLG (2003)
	Previous Method	Present Method	Previous Method	Present Method	
P_S	0.2698	0.2509	0.1901	0.1707	0.1667
O_{MS} (m^3)	4889.2	4546.7	3444.9	3093.4	3020.5

8.7 Remarks

The structural designer would be more interested in obtaining a quick tool for assessing a structural design for various accident scenarios. A new simplified analytical model for predicting the impact force and the dissipated energy caused by the side structure damage, transverse vibration and global motions of struck ship is derived. The emphasis has been on the dynamic effect of struck ship during collision procedure.

The new simplified analytical method takes collision velocity, collision angle and collision location into account, and can be used for a wide range of different accident scenarios. Calculations using this method compared satisfactorily with FEM simulation results. Through benchmark studies, the new simplified analytical mechanics model has proved to a rational practical simplified design oriented procedure for ship side collision on the initial stage of oil tanker design. This method can be easily incorporated into a probability-based framework to properly assess structural performance for a variety of damage scenarios.

Application of new simplified method to mean oil outflow estimation is performed. Combined with PDF assumption of collision angles and striking velocity proposed by Brown, the present method can predict more reasonable result of mean oil outflow.

The new simplified analytical method developed, and the results and insights obtained by the present study should be useful for the rational design of double hull tanker side structures against ship collision to reduce the risk of oil pollution and for the collision resistance evaluation of existing double hull tanker structures.

Chapter 9 Conclusion and Suggestions for Future Research

9.1 Conclusion

The main objective of this thesis is to establish the rational procedure to evaluate the structural damage, energy dissipation and striking/struck ship motion correctly in case of liquid products tanker's collision and grounding. The Arbitrary Langrangian Eulerian (ALE) finite element method, which can consider the fluid-structure interactions of liquid products in tank and surrounding water, can improve the accuracy and reliability of nonlinear finite element method for liquid cargo ship collision and grounding simulation.

The crushing collapse of thin-walled structure elements is the most important failure modes during head-on collision. Since nonlinear finite element method becomes a powerful tool in ship collision and grounding problem analysis, a study on the crushing collapse of stiffened square tube using nonlinear FEM was performed. By comparing the experimental data with FEM simulation results, the new equivalent plate thickness formulas for the longitudinally stiffened square tube, transversely stiffened square tube and orthogonally stiffened square tube are derived, respectively. The predicting result of the mean crushing load using the new equivalent plate thickness formulas is in fair agreement with the experiment data.

To improve computing efficiency, accuracy and stability of nonlinear FEM, the effect of selected parameters on crashworthiness of the single-hull bottom structure is investigated. The effect of boundary condition, different shell element types, the residual stress, the material model, the friction coefficient, the rupture strain was discussed.

Through validation of the ALE FE method on the rectangular tank sloshing experiment and the sway motion of hull experiment, the ALE FE method is proved to be suitable to simulate the fluid-structure interaction of liquid cargo in tank and the surrounding water.

Four different numerical FE models for liquid cargo in tank were performed. The advantage of ALE FE method is that it can accurately simulate the fluid-structure interaction in liquid cargo tank. However the CPU time of this method is much larger than other three FE models. On the other hand, although the Linear Sloshing FE model and Rigid Point Mass model need the shortest CPU time, these FE model underestimate or neglect the hydrodynamic force in liquid cargo tank. Compared to the result of ALE FE model, the Lagrangian FE model is appropriate for predicting the structure behavior of

damaged struck cargo tank accounting for the fluid-structure interaction in liquid cargo tank with reasonable accurateness and a relatively low required CPU time.

Numerical simulation of the ship collision between a 350,000 tonne VLCC collide with a 293,000 tonne double hull VLCC, taking account of both fluid-structure interaction in liquid tank and surrounding water, was performed. In order to improve the accuracy of collision behavior of struck ship under the defined collision scenarios, the effect of collision angle, the striking ship velocity, the mass of the striking ship and struck ship velocity, is discussed.

For a reliable and practical evaluation of structural response of side collision, a new simplified analytical internal mechanics model is proposed, which the dynamic effect including transverse vibration and global motions of struck ship on the impact force are considered. Application of present simplified method, estimation oil outflow in side collision is carried out. The mean oil outflow for side impact can be efficiently and accurately evaluated by assuming appropriate PDF of collision angle, impact location and striking velocity model, and assembling the new simplified analytical model.

9.2 Suggestions for Future Research

Currently, there are no widely or generally accepted ship collision and grounding design standards. Design standards should be developed by the community, which should be consisted of classification societies, international organizations (ISO, IMO), leading researchers in the field, representatives from the ship design and shipbuilding communities, ship owners and operators, professional societies, governments and regulators. We should establish a more rational predictive calculation approaches on crashworthiness and safety. Further in-depth studies are needed to investigate the behavior of aluminum and sandwich panels, and innovative designs that maximize the crashworthiness in an accidental impact.

The primary failure modes of plates in ship collision and grounding, such as tearing of plate, concertina tearing of plate, denting of plate, penetration of plate and stretching of plate, should be studied using nonlinear FEM. The effect of geometry of stiffener or indenter can be investigated deeply.

The reliable automated simulation of the structural failure process up to occurrence of fracture in ship collision and grounding is probably the most challenging task in applying

nonlinear FEM. For typical ship structures the stress state is tri-axial which complicates the development of proper failure criteria for rupture. There are various approaches presented to handle the tri-axial failure criteria for rupture. Still the validation of the available approaches is fairly limited especially with real structural configurations. Especially the proper modeling method of the rupture in nonlinear FE-analysis needs further studies.

The element kill algorithm can be coupled with the stiffness reduction and is sometimes a useful method in simulations of fracture initiation and crack propagation duo to the simplicity and cost effectiveness. When an element has reached the failure criterion value, the element is deleted from the calculation. This will often cause elastic stress waves in the structure as the stiffness is suddenly reduced. The so-called mesh-free new numerical methods for simulating crack propagation, where problems with distorted elements are somewhat avoided, should be further studies.

Moreover, the effects of including the welds in simulations of ship collision and grounding should be studied.

Appendix

A1. The Explicit and Implicit Method

Two types of FE methodologies, implicit and explicit techniques, are used to solve the nonlinear problems.

Define the semi-discrete equation of motion is:

$$M\ddot{x}(t) + F_{\text{int}}(x, \dot{x}) - F_{ext}(x, t) = 0 \tag{A-1}$$

where

$\ddot{x}, \dot{x}, x$ the acceleration, velocity, coordinate vectors

M the diagonal mass matrix

F_{ext} the external load and body force vector

F_{int} the stress divergence vector

In order to briefly explain, assumption that the F_{int}^{n} is linear is made

$$F_{\text{int}}(x, \dot{x}) = C\dot{x} + K\Delta x \tag{A-2}$$

where

K the stiffness matrix

C the damping matrix

Δx the displacement vector

Regardless of whether an explicit or implicit integration scheme is used, we require that

$$Q = M\ddot{x} + C\dot{x} + K\Delta x - F_{ext} = 0 \tag{A-3}$$

Explicit integration trivially satisfies these equations since the calculation of the acceleration guarantees equilibrium

$$\ddot{x}^{n} = M^{-1}\left(F_{ext}^{n} - F_{\text{int}}^{n}\right) = M^{-1}\left(F_{ext}^{n} - C\dot{x} - K\Delta x\right) \tag{A-4}$$

Using central difference integration, the explicit update of the velocities and coordinates is given by

$$\dot{x}^{n+1/2} = \dot{x}^{n-1/2} + \ddot{x}^{n}\Delta t^{n} \tag{A-5}$$

$$x^{n+1} = x^{n} + \dot{x}^{n+1/2}\Delta t^{n+1/2} \tag{A-6}$$

where

$$\Delta t^{n+1/2} = \frac{\left(\Delta t^{n} + \Delta t^{n+1}\right)}{2} \tag{A-7}$$

Stability places a limit on the time size. This step size may be very small and a large number of steps may be required.

For the implicit solution, the residual vector Q becomes an implicit function of x^{n+1} only. We seek the vector x^{n+1} such that

$$Q\left(x^{n+1}\right) = 0 \tag{A-8}$$

Assume an approximation x_k^{n+1} to x^{n+1} for $k = 1,2,3\ldots$ etc. In the neighborhood of x_k^{n+1}, the linear approximation to $Q\left(x^{n+1}\right) = 0$ is given by

$$Q\left(x_k^{n+1}\right) = Q\left(x_{k-1}^{n+1}\right) + J\left(x_{k-1}^{n+1}\right)\Delta x_k = 0 \tag{A-9}$$

And iterate for the solution:

$$J\left(x_{k-1}^{n+1}\right) = \frac{\partial Q}{\partial x}\Big|_{x_{k-1}^{n+1}} \tag{A-10}$$

The Jacobian matrix is expressed as

$$J = M\frac{\partial \ddot{x}}{\partial x} + C\frac{\partial \dot{x}}{\partial x} + K - \frac{\partial F_{ext}}{\partial x} \tag{A-11}$$

The solution of increment in displacement is

$$\Delta x_k = -\left(J\left(x_{k-1}^{n+1}\right)\right)^{-1} Q\left(x_{k-1}^{n+1}\right) \tag{A-12}$$

$$x_k^{n+1} = x_{k-1}^{n+1} + \Delta x_k \tag{A-13}$$

If convergence is not satisfied, the displacement vector is updated

$$x_{k+1}^{n+1} = x_k^{n+1} + \Delta x_{k+1} \tag{A-14}$$

And another iteration is performed.

The implicit solvers are properly applied to static, quasi-static, and dynamic problems with a low frequency content. An advantage of the implicit solver than explicit integration is that the number of load or time steps is typically 100 to 10000 times fewer. The major disadvantage is that the cost per step is unknown since the speed depends mostly on the convergence behavior of the equilibrium iterations which can vary widely from problem to problem. The calculation cost depends largely on the number of equations in system and the computer capacity, especially memory resources.

A2. The Time Integration

During the solution we loop through the elements to update the stress vector and determine a new time step size by taking the minimum value of all elements

$$\Delta t^{i+1} = \alpha \cdot \min\{\Delta t_1, \Delta t_2, \Delta t_3, \ldots \Delta t_N\} \tag{A-15}$$

where

Δt the time step

N the total number of elements

α the scale factor, 0.9 or less

The time step calculation for shell elements is as follows.

$$\Delta t_e = \frac{L_s}{C} \tag{A-16}$$

where

L_s the characteristic length

$$L_S = \frac{A_S}{\max(L_1, L_2, L_3, L_4)} \tag{A-17}$$

C the sound speed

$$C = \sqrt{\frac{E}{\rho(1-\gamma^2)}} \tag{A-18}$$

where

A_s the element area

L_1, L_2, L_3 and L_4 the lengths of the element sides

E Young's modulus

ρ the density

γ Poisson's ratio

A3. The Effect of Strain Rate

With the increase in the strain rate, the yield stress of material increases, while the ductility is reduced. The most commonly adopted formula to deal with the strain rate sensitivity on yield stress is one proposed by Cowper and Symonds (1957), which is given by

$$\frac{\sigma_{yd}}{\sigma_y} = 1.0 + \left(\frac{\dot{\varepsilon}}{C}\right)^{1/q} \tag{A-19}$$

where

C, q coefficients to be determined based on test data

σ_y the static yield stress

σ_{yd} the dynamic yield stress

$\dot{\varepsilon}$ the strain rate

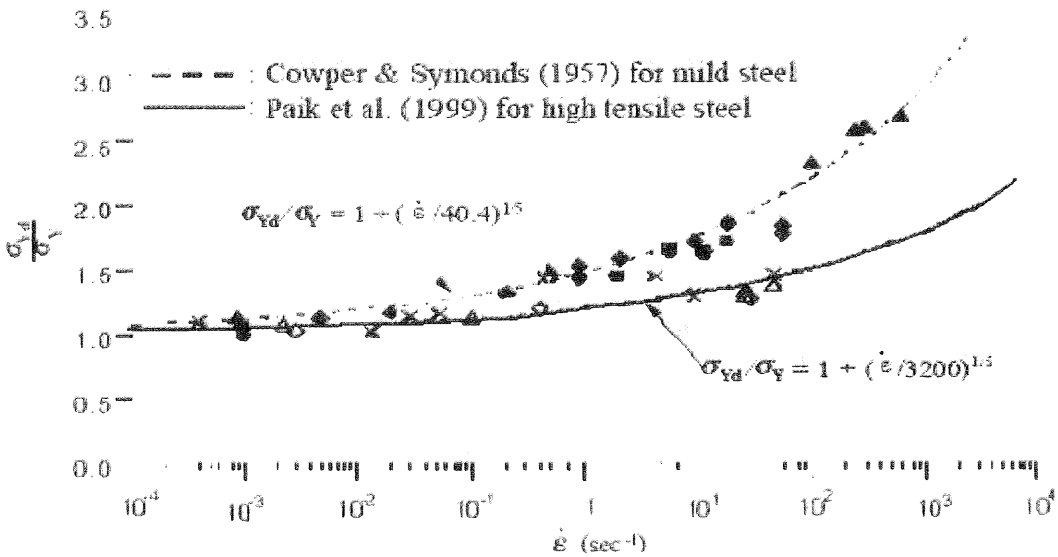

Fig. A. 1 Yield strength versus strain rate for mild and high tensile steels (ISSC 2003)

Figure A.1 plots the Cowper-Symonds formula together with the relevant coefficients for mild or high tensile steels. It is seen from Fig. A.1 that as the strain rate increases the dynamic yield stress increases. It is also found that for higher tensile steel the percentage increase of the ratio of the dynamic yield stress to the static yield stress is smaller than that for mild steel. It is noted that the Cowper-Symonds formula relates to yield stress; the strain rate dependence is smaller for the flow stress at large strains.

The following approximate formula, which is the inverse of the Cowper-Symonds formula for the dynamic yield stress, is then useful for estimating the dynamic fracture strain as a function of the strain rate (Jones 1989), namely

$$\frac{\varepsilon_{Fd}}{\varepsilon_F} = \left[1.0 + \left(\frac{\dot{\varepsilon}}{C}\right)^{1/q}\right]^{-1} \tag{A-20}$$

where

ε_{Fd} the static fracture strain

ε_F the dynamic fracture strains

A4. Shell Element Formulation

Shell elements are the main element type in crashworthiness simulation. The advantage of using 3-d elastic-plastic shell elements in finite element simulation is that the solution includes membrane bending effects, history dependence and also handles contact-friction problem quit easily. Thus the shell element is possible to simulate large complex structures with high accuracy.

The shell elements may differ in sharp and the integration rule. Fully integrated four-node quadrilaterals use four integration points in-plane. Under-integrated elements only use one integration point in the plane. In under-integrated shell elements, the strain is evaluated at the element centre and results in the element to exhibit zero energy modes (hourglass modes) where the elements can deform without dissipating energy. Figure A.2 shows the hourglass modes of solid element. Fully integrated elements do not have these hourglass problems, but they may lock in shear which will cause the element to exhibit excessive stiffness.

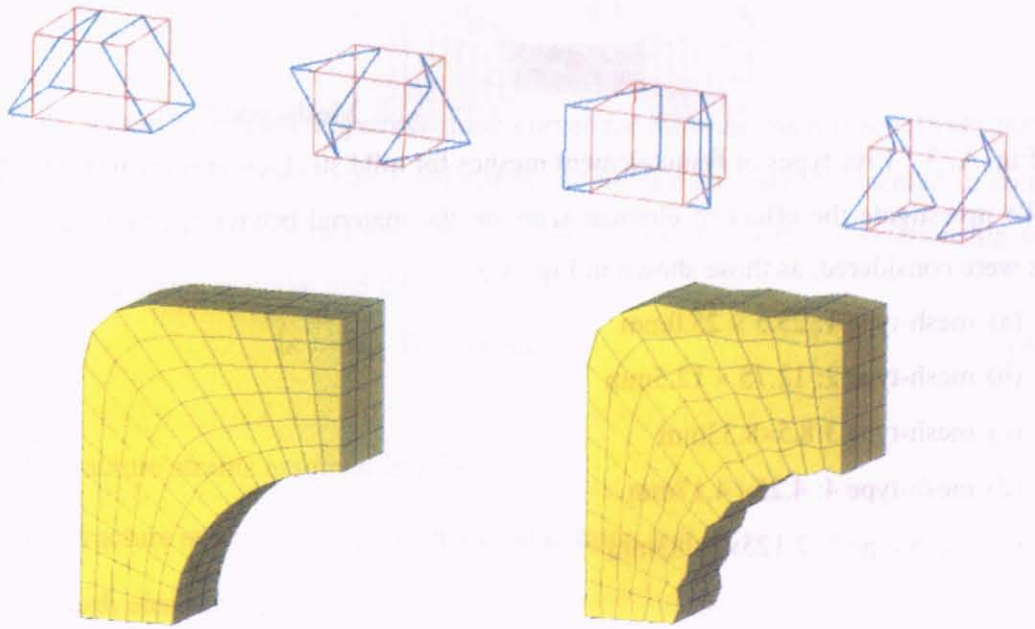

Fig. A. 2 Hourglass modes of solid elements

A5. Relationship Between the Mesh Size and Rupture Strain

Traditionally, rupture is assumed to occur when the equivalent plastic strain in an analyzed structure reaches a critical value. This critical value, sometime referred to as rupture strain, is related to the strain-stress curves obtained from mechanical tests of uni-axially stretched metal coupons. There has been an interest in defining rupture strain for FEM analyses. The dependency of fracture strain on element size has been studied by Yu (1996), Lehmann and Yu (1998b) and Simonsen and Lauridsen (2000). ISSC (2003) reported a benchmark study on a tensile coupon test of a flat mild steel specimen to investigate the dependency of the input fracture strain on element size.

The stress-strain curve for a tensile coupon test on flat mild steel specimen (thickness of 2mm) in a quasi-static condition was computed using the nonlinear finite element program LS-DYNA. The Belytschko-Tsay type plate-shell elements with a piecewise-linear plasticity material model were employed.

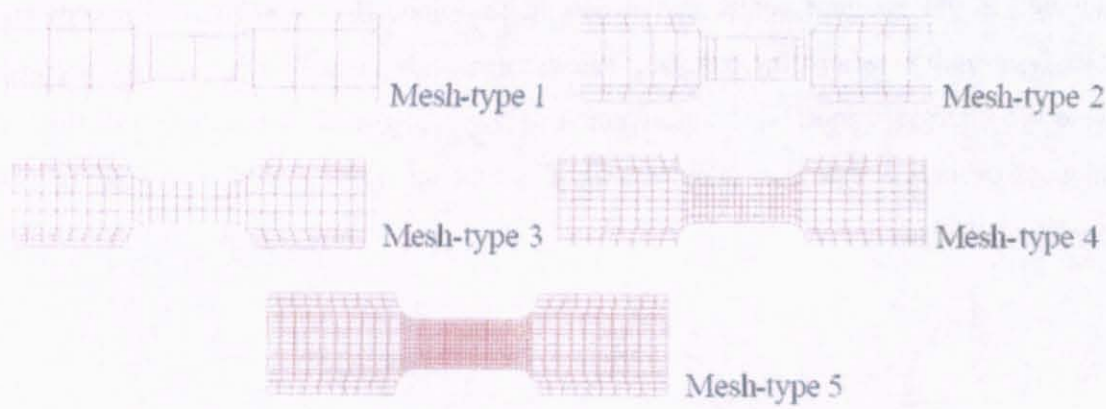

Fig. A. 3 Five types of finite element meshes for mild steel test specimen (ISSC 2003)

To investigate the effect of element sizes on the material behavior, five types of element sizes were considered, as those shown in Fig. A.3.

(a) mesh-type 1: 25.5 × 25.0mm

(b) mesh-type 2: 12.75 × 12.5mm

(c) mesh-type 3:8.5×8.33mm

(d) mesh-type 4: 4.25× 4.17mm

(e) mesh type 5: 2.125×2.083mm

Figure A.4 compares the finite element solutions with the test in terms of the engineering

stress-strain relationship. It is seen from Fig. A.4 that prediction results with different mesh size overestimates the strain hardening effect. Figure A.5 shows the input fracture strains which were obtained by a trial and error technique so that the "critical" fracture strains by FEA corresponded to those by testing. It is interesting to note that this correspondence was achieved by assuming different level of the fracture strain in the FEA with different meshes.

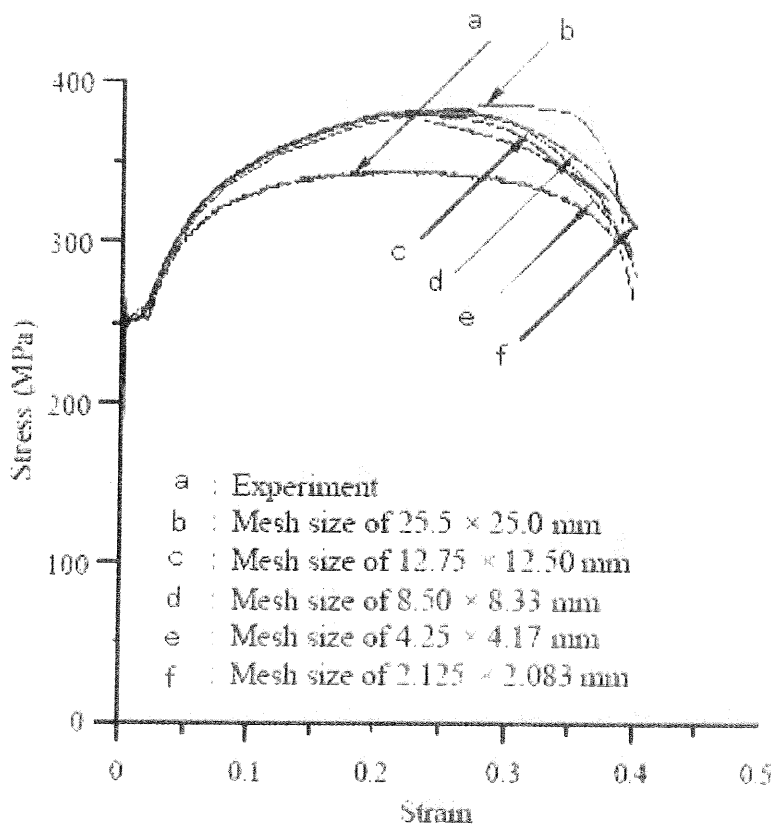

Fig. A. 4 Result of engineering stress-strain curves for different mesh types (ISSC 2003)

The fracture strain – element size relationship can be approximately presented in equation (A-21) to match the findings of this benchmark study. However, a different relationship would be expected for different material and thickness

$$(\varepsilon_f - \varepsilon_{f0})S = \text{constant} \tag{A-21}$$

where

ε_f the fracture strains assumed in FEA

ε_{f0} the fracture strains obtained by material coupon test

S the mesh element size

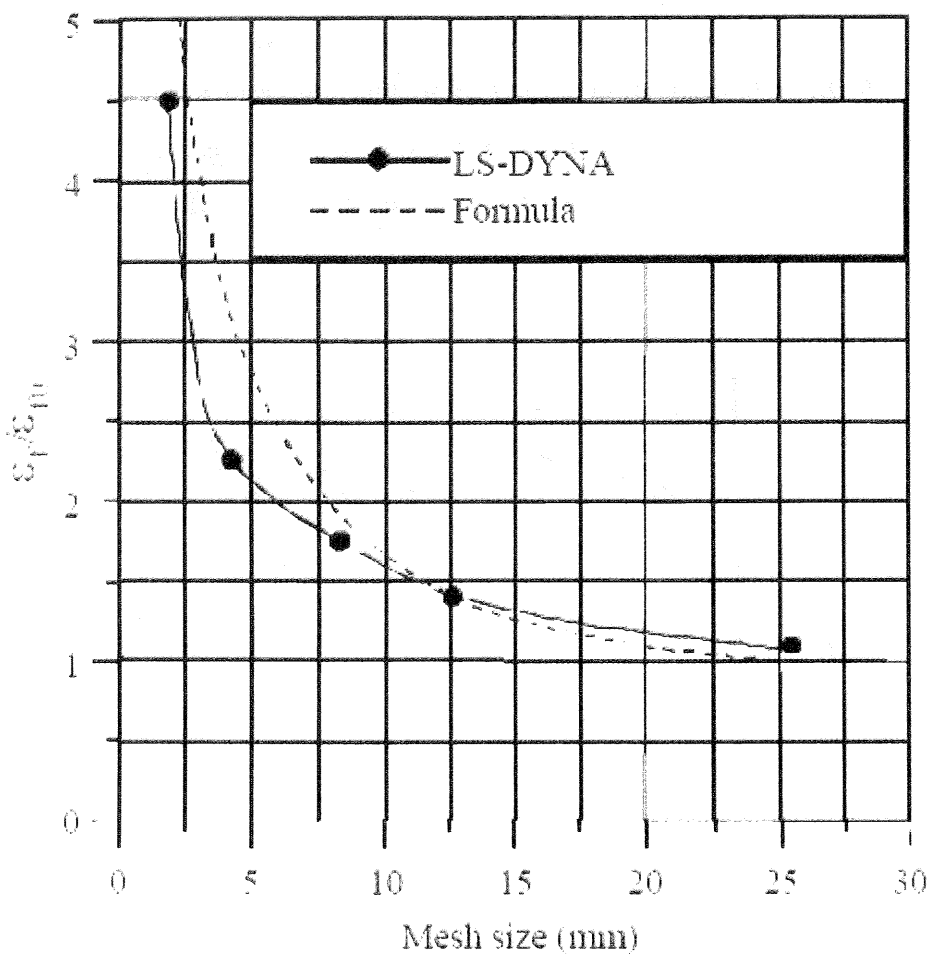

Fig. A. 5 Normalized 'critical' fracture strain VS the finite element size (ISSC 2003)

By comparing tensile tests with numerical simulations they concluded that a fairly small element mesh is required to capture the features of the tensile test.

Ranges of rupture strain were studied by Simonsen and Törnqvist (2004), Okazawa et al., (2004), Yamada et al. (2005), Alsos and Amdahl (2005). Refined simulation of fracture initiation and propagation requires that mesh size are small enough. This in turn makes the analysis of large ship structures very time consuming and computational demanding.

A6. Arbitrary Lagrangian-Eulerian (ALE) Formulation

In this section, ALE formulation, as implemented in LS-DYNA Keyword Manual 970(2003), is briefly outlined.

In the ALE description, an arbitrary referential coordinate is introduced in addition to the Lagrangian and Eulerian coordinates. The ALE equations are derived by substituting

the relationship between the material time derivative and the reference configuration time derivative,

$$\frac{\partial f(X_i,t)}{\partial t} = \frac{\partial f(x_i,t)}{\partial t} + (v_i - u_i)\frac{\partial f(x_i,t)}{\partial x_i} = \frac{\partial f(x_i,t)}{\partial t} + w_i \frac{\partial f(x_i,t)}{\partial x_i} \qquad \text{(A-22)}$$

where

X_i the Lagrangian coordinate

i the referential coordinate

x_i the Eulerian coordinate

v_i the material velocity

u_i the mesh velocity

In order to simplify the equations, we introduce the convective velocity $w_i = v_i - u_i$.

Thus the governing equations for the ALE formulation are given by:

(i) The conservation of mass equation.

$$\frac{\partial \rho}{\partial t} = -\rho \frac{\partial v}{\partial x_i} - w_i \frac{\partial \rho}{\partial x_i} \qquad \text{((A-23)}$$

(ii) The conservation of momentum equation.

$$\rho \frac{\partial v_i}{\partial t} + \rho w_i \frac{\partial v_i}{\partial x_j} = \sigma_{ij,j} + \rho b_i \qquad \text{((A-24)}$$

(iii) The conservation of total energy equation

$$\rho \frac{\partial E}{\partial t} + \rho w_j \frac{\partial E}{\partial x_j} = \sigma_{ij} v_{i,j} + b_j v_j \qquad \text{((A-25)}$$

where

ρ the density

b_i the body force

E the energy

The overall flow of an ALE time step is as follows

1. perform a Lagrangian time step
2. perform an advection step
   a) decide which nodes to move
   b) move the boundary nodes

c) move the interior nodes

d) calculate the transport of the element-centred variables

e) calculate the momentum transport and update the velocity

It is should be noted that the cost of the advection step per element is usually much larger than the cost of Lagrangian step. Most of the time in the advection step is spent on calculating the material transported between the adjacent elements, and only a small part of it is spent on calculating how and where the mesh should be adjusted. Second order accurate monotonic advection algorithms are used in LS-DYNA because of their superior coarse mesh accuracy with few elements.

At ALE-Lagrange interface, the Lagrange mesh acts as a moving boundary to the fluid, while fluid pressure is applied to the Lagrange mesh. Using penalty coupling allows us to treat the impact problems in presence of fluid because penalty coupling manages the interactions between a Lagrangian formulation modeling the structure and a ALE formulation modelling the fluid to flow around a structure but not through a structure. Flow through the structure is prevented in an approximate way by applying penalty forces to the fluid and structure. As soon as an ALE node penetrates in a Lagrangian structure, a force of recall is exerted on the contravening node and put its back on the surface of the structure.

More accurately, first, for each Lagrangian node, a search of an ALE element containing this node is done. Then, the penetration depth of each fluid node into the structure surface is evaluated. Finally, penalty forces are determined proportionally to the penetration depth. The coupling method behaves like a spring system.

A7. Fluid-like Material Model

In commercial FE code LS-DYNA, the Constitutive Model and Equation of State are used to describe fluid-like material model with fluid-like deformation characteristics (air, water, oil etc.).

Constitutive Model (CM) relates σ'_{ij} to ε'_{ij}

$$\sigma^{v}{}_{ij} = \sigma'_{ij} = \gamma \cdot \dot{\varepsilon}'_{ij} \tag{A-26}$$

where

$\dot{\varepsilon}'_{ij}$ the deviatoric strain rate (1/s)

γ the dynamic viscosity (Pa*s)

The dynamic viscosity of crude oil is $1.019 \times 10^{-5} N/m^2 * s$

Equation of State (EOS) relates the pressure (P) to the specific rate of change of volume ($\Delta v / v$) of a material at a physical state. For fluid (water, crude oil etc), the EOS is given by:

$$P = K\mu \tag{A-27}$$

where

$$\mu = -\frac{\Delta v}{v} = \frac{\rho}{\rho_0} - 1 \tag{A-28}$$

$\frac{\rho}{\rho_0}$ the ratio of current density to initial density

K the bulk modulus.

The bulk modulus of crude oil is $1.455 \times 10^9 \ N/m^2$

The total stress in the fluid-like material is

$$\sigma_{ij} = \sigma'_{ij} + \frac{1}{3}\sigma_{kk}\delta_{ij} = \gamma \cdot \dot{\varepsilon}'_{ij} - P\delta_{ij} \tag{A-29}$$

A8. Calculation of Added Mass Coefficients

The hydrodynamic force related to the surge motion of ship is very small compared to sway force. The hydrodynamic forces related to the surge motion cannot be found by strip method. The sectional surge added mass $A_{1,1}$ related to the forward motion is small compared with the mass of the ship. Professor Motora (1969) found it to be $(0.02 - 0.07)M$. A reasonable assumption may be

$$A_{1,1} = 0.05M \tag{A-30}$$

Many researchers have proposed different methods to evaluate the sectional sway added mass coefficients for ship forms; the pioneer works being that by Lewis F. M. (1929), Tasai F. (1961). The sway hydrodynamic added mass coefficient at infinite frequency using Lewis Two Parameter Conformal Mapping Method to be given by

$$A_{2,2} / M = \frac{2\rho}{\pi}\{D^2 + \frac{16}{3}a_3{}^3\} \tag{A-31}$$

where

$$a_3 = \frac{-c_1 + 3 + (9 - 2c_1)^{1/2}}{c_1} \tag{A-32}$$

$$c_1 = [3 + \frac{4\sigma_S}{\pi}] + [1 - \frac{4\sigma_S}{\pi}][(H_O - 1)/(H_O + 1)]^2 \tag{A-33}$$

$$H_O = \frac{B}{2D} \qquad \sigma_S = \frac{A_S}{DB} \tag{A-34}$$

B and D is the breadth and draught of cross section, respectively

A_s is wetted area of cross section

The added mass coefficient for the pitch/yaw motion of ship, $A_{5,5} / A_{6,6}$, is (Pedersen et al.,1993)

$$A_{5,5} = 0.21 \cdot I_{yy} \tag{A-35}$$

$$A_{6,6} = 0.21 \cdot I_{zz} \tag{A-36}$$

A9. Calculation of Mean Oil Outflow for Side Damage

As the method in BLG 8/18/Add.1 given, the mean oil outflow for side damage shall be calculated as follows:

$$O_{MS} = C_3 \sum_{i=1}^{n} P_S(i) O_S(i) \qquad (m^3) \tag{A-37}$$

where

O_{MS} mean outflow for side damage, in m^3

i represents each cargo tank under consideration

n total number of cargo tanks

$P_S(i)$ the probability of penetrating cargo tank i from side damage

$O_S(i)$ the outflow from side damage to cargo tank i, which is assumed equal to the total volume in cargo tank i, in m^3,

C_3 0.77 for special VLCC, or 1.0 for all other ships

The probability PS of breaching a compartment from side damage shall be calculated as follows:

$$P_S = P_{SL} \cdot P_{SV} \cdot P_{ST} \qquad \text{(A-38)}$$

where

$P_{SL} = 1 - P_{Sf} - P_{Sa}$ probability the damage will extend into the longitudinal zone bounded by X_a and X_f

$P_{SV} = 1 - P_{Su} - P_{Sl}$ probability the damage will extend into the vertical zone bounded by Z_l and Z_u

$P_{ST} = 1 - P_{Sy}$ probability the damage will extend transversely beyond the boundary defined by y

P_{Sa}, P_{Sf}, P_{Sl}, P_{Su} and P_{Sy} shall be determined by linear interpolation from the table of probabilities for side damage provided in this regulation.

where

P_{Sa} the probability the damage will lie entirely aft of location X_a / L

P_{Sf} the probability the damage will lie entirely forward of location X_f / L

P_{Sl} the probability the damage will lie entirely below the tank

P_{Su} the probability the damage will lie entirely above the tank

P_{Sy} the probability the damage will lie entirely outboard of the tank

Compartment boundaries X_a, X_f, Z_l, Z_u and y shall be developed as follows:

X_a the longitudinal distance from the aft terminal of L to the aftmost point on the compartment being considered, in metres

X_f the longitudinal distance from the aft terminal of L to the foremost point on the compartment being considered, in metres

Z_l the vertical distance from the moulded baseline to the lowest point on the compartment being considered, in metres

Z_u the vertical distance from the moulded baseline to the highest point on the compartment being considered, in metres

y the minimum horizontal distance measured at right angles to the

centreline between the compartment under consideration and the side shell in metres

P_{Sy} shall be calculated as follows:

$$P_{Sy} = \begin{cases} \left(24.96 - 199.6\frac{y}{B}\right)\cdot\frac{y}{B} & for\ \frac{y}{B} \le 0.05 \\ 0.749 + \left[5 - 44.4\left(\frac{y}{B} - 0.05\right)\right]\left(\frac{y}{B} - 0.05\right) & for\ 0.05 < \frac{y}{B} < 0.1 \\ 0.888 + 0.56\left(\frac{y}{B} - 0.1\right) & for\ \frac{y}{B} \ge 0.1 \end{cases} \qquad \text{(A-39)}$$

P_{Sy} shall not be taken greater than 1.

Table A-1 Probabilities for Side Damage

X_a / L	P_{Sa}	X_f / L	P_{Sf}	Z_l / D	P_{Sl}	Z_u / D	P_{Su}
0.00	0.000	0.00	0.967	0.00	0.000	0.00	0.968
0.05	0.023	0.05	0.917	0.05	0.000	0.05	0.952
0.10	0.068	0.10	0.867	0.10	0.001	0.10	0.931
0.15	0.117	0.15	0.817	0.15	0.003	0.15	0.905
0.20	0.167	0.20	0.767	0.20	0.007	0.20	0.873
0.25	0.217	0.25	0.717	0.25	0.013	0.25	0.836
0.30	0.267	0.30	0.667	0.30	0.021	0.30	0.789
0.35	0.317	0.35	0.617	0.35	0.034	0.35	0.733
0.40	0.367	0.40	0.567	0.40	0.055	0.40	0.670
0.45	0.417	0.45	0.517	0.45	0.085	0.45	0.599
0.50	0.467	0.50	0.467	0.50	0.123	0.50	0.525
0.55	0.517	0.55	0.417	0.55	0.172	0.55	0.452
0.60	0.567	0.60	0.367	0.60	0.226	0.60	0.383
0.65	0.617	0.65	0.317	0.65	0.285	0.65	0.317
0.70	0.667	0.70	0.267	0.70	0.347	0.70	0.255
0.75	0.717	0.75	0.217	0.75	0.413	0.75	0.197
0.80	0.767	0.80	0.167	0.80	0.482	0.80	0.143
0.85	0.817	0.85	0.117	0.85	0.553	0.85	0.092
0.90	0.867	0.90	0.068	0.90	0.626	0.90	0.046
0.95	0.917	0.95	0.023	0.95	0.700	0.95	0.013
1.00	0.967	1.00	0.000	1.00	0.775	1.00	0.000

Bibliography

Akita Y., Ando N., Fujita Y. & Kitamura K.(1972). Studies on collision-protective structures in nuclear-powered ships. Nuclear Engineering and Design, 19: pp.365-401.

Alexander W. J., Gielen Alex W., et al.(2004). Response of stiffened plate panels to hydrodynamic impact-Theory and experiments. PRADS 2004.

Alsos H. S. & Amdahl J.(2005). Intentional grounding of disabled ships, Marine 2005 –Computational Methods in Marine Engineering, Oslo, Norway, pp.27-29, June 2005.

Amdahl J.(1983). Energy absorption in ship-platform impact, Norway Institute of Technology, Report No. UR-83-84.

ASIS(1993). Prediction methodology of tanker structural failure & consequential oil spill , Technical Report, Japan.

Brown A.(2002). Collision scenarios and probabilistic collision damage, International Conference on Collision and Grounding of Ships (ICCGS), pp.259-272, Copenhagen, Denmark.

Brown A.(2002). Modelling Structural Damage in Ship Collisions, SSC-422, Ship Structure Committee.

Cowper G. R. & Symonds P. S.(1957). Strain-hardening and strain rate effects in the impact loading of cantilever beams, Brown University, Technical Report No. 28.

Endo H.(2004). Rationalization in the probabilistic method estimating the mean oil outflow for side damage, International Conference on Collision and Grounding of Ships (ICCGS), pp.182-187, Izu, Japan.

Endo H. & Yamada Y.(2001). The Performance of Buffer Bow Structures against Collision (1st Report: Collapse Strength of the Simplified Structure Models. Journal of the Society of Naval Architects of Japan, Vol. 189, pp.209-217.

Endo H., Yamada Y. & Hashizume Y.(2005). The Performance of Buffer Bow Structures against Collision (2nd Report: The Effect in Preventing Oil Outflow. Journal of the Society of Naval Architects and Marine Engineers of Japan, Vol. 2, pp.351-360.

Endo H., Yamada Y. & Kawano H.(2004). Verification on the effectiveness of buffer bow structure through FEM simulation. 3rd International Conference on Collision and Grounding of Ships (ICCGS), pp.151-159, Izu, Japan.

Han S. M., Ito H. & Suh Y. S.(2005). Collision analysis using analytical approach, International Offshore and Polar Engineering Conference (ISOPE), Seoul, Korea, pp.19-24, June 2005.

Housner G. W.(1957). Dynamic pressure on accelerated fluid containers, Bulletin of the Seismological Society of America, Vol. 47, pp.15-35.

Hu Z., Gu Y., Gao Z. & Li Y.(2005). Fast evaluation of ship-bridge collision force based on nonlinear numerical simulation (in Chinese), Engineering Mechanics, 22:3, pp.235-240.

IMO BLG (2003) Annx 5 Draft Revised MARPOL Annex 1

ISSC(2003). Committee V.3 Collision and Grounding. 15th International Ship and Offshore Structures Congress(ISSC), San Diego, August.

ISSC(1983). Committee II.4 Steady state loading and response. 8th International Ship and Offshore Structures Congress

Ito H., Kondo K., Yoshimura N., Kawashima M. & Yamamoto S.(1984). A simplified method to analyse the strength of double hulled structures in collision, Journal of SNAJ, 156, pp.299-312.

Ito H., Kondo K., Yoshimura N., Kawashima M. & Yamamoto S.(1986). A simplified method to analyse the strength of double hulled structures in collision (3rd Report), Journal of SNAJ, 160, pp.401-409.

J. M. J. Journée(1993). Hydromechanic Coefficients for Calculating Time Domain Motions of Cutter Suction Dredges by Cummins Equations, Report 0968, The Netherlands.

Jastrzebski T., Taczala M. & Grabowiecki K.(2004). Numerical simulation of cash and grounding of inland waterway transportation barges, International Symposium on Practical Design of Ships and other Floating Structures (PRADS), Luebeck-Travemuende, Germany, pp.12-17, September 2004.

Jiang H. & Gu Y.(2004). Study on ship collisions and buffer bow structures, 3rd International Conference on Collision and Grounding of Ships (ICCGS), pp.25-27, October 2004, Izu, Japan.

Jones N.(1989). On the dynamic inelastic failure of beams, Chapter 5 in Structural Failure, John Wiley &Sons, New York, pp.133-159.

Jones N. & Birch R. S.(1990). Dynamic and static axial crushing of axially stiffened square tubes Proceedings Institute of Mechanical Engineers, 204(C), pp.293-295.

Kajaste-Rudnitski J., Varsta P.M. & Matusiak J. E.(2004a). Dynamics of ship grounding, International Symposium on Practical Design of Ships and other Floating Structures (PRADS), Luebeck-Travemuende, Germany, pp.12-17, September 2004.

Kajaste-Rudnitski J., Varsta P.M. & Matusiak J. E.(2004b). Mechanics of ship grounding, International Offshore and Polar Engineering Conference (ISOPE), pp.569-576, Toulon, France.

Kajaste-Rudnitski J., Varsta P. & Matusiak J.(2005). Some finite element estimates of ship collision event, 447-453, International Congress of International Maritime Association of the Mediterranean (IMAM), Lisboa, Portugal, pp.26–30, September.

Kitamura O.(1999). Comparative study on collision resistance of side structure, Marine Technology, 34:4, pp.292-308.

Kitamura O.(2001). FEM approach to the simulation of collision and grounding damage. The second International Conference on Collision and Grounding of ships. Copenhagen, Denmark, July 1-3.

Kitamura O., Kuroiwa T., Kawamoto Y. & Kaneko E.(1998). A Study on the Improved Tanker Structure against Collision and Grounding Damage. Proceedings of the 7th PRADS, pp.173-179.

Klanac A., Ehlers S., Tabri K., Rudan S. & Broekhuijsen J.(2005). Qualitative design assessment of crashworthy structures, International Congress of International Maritime Association of the Mediterranean (IMAM), Lisboa, Portugal, pp.26–30, September 2005.

Konter A., Broekhuijsen J. & Vredevelt A.(2004). A quantitative assessment of the factors contributing to the accuracy of ship collision predictions with finite element method, 3rd International Conference on Collision and Grounding of Ships (ICCGS), Izu, Japan, pp.25-27, October 2004.

Krzysztof W. & Przemyslaw K.(2003). The effect of selected parameters on ship collision results by dynamic FE simulations, Finite Elements in Analysis and Design vol. 39, pp.985 - 1006.

Kuroiwa T.(1996). Numerical simulation of actual collision and grounding experiments. International Conference on Design and Methodologies for Collision and Grounding Protection of Ships, San Francisco.

Landweber L. & Macagno M.(1957). Added mass of two-dimensional forms oscillating in a free surface. Journal of Ship Research, pp.20-30, November.

Laubenstein L., Mains C., Jost A., Tagg R. & Bjoerneboe N.(2001). Updated probabilistic extents of damage based on actual collision data, Proceedings of ICCGS'01, Copenhagen, pp.93-99.

Le Sourne H., Couty N., Besnier F., Kammerer C. & Legavre H.(2003). LS-DYNA applications in shipbuilding, 4th European LS-DYNA Users Conference, A:II, pp.1-16.

Lee J. W. & Choung J. M.(1996). Energy dissipation and mean crushing strength of stiffened plates in crushing . Journal of Hydrospace Technology, Society of Naval Architects of Korea, 2, pp.27-40.

Lehmann E. & Biehl F.(2004). Collision of ships and offshore wind turbines: calculation and risk evaluation, International Conference on Collision and Grounding of Ships (ICCGS), Izu, Japan, October 2004.

Lehmann E. & Yu X.(1998b). On ductile rupture criteria for structural tear in the case of shi p collision and grounding, Proceedings of PRADS'98, The Hague, pp.149-156.

Lewis F. M.(1929). The inertia of the water surrounding a vibrating ship.Trans. SNAME, 37: pp.1-20.

Li X.(1999). The strength evaluation of bridge pier collided by ship (In Chinese). Railway Standard Design, 19:2, pp.8-13.

Liang W., Jin Y. & Chen G.(2000). Study on the determination of force for ship-bridge collision and protective device (in Chinese), The Fourteenth Chinese Bridge Academy Conference, pp.566-571.

Liu J. & Gu Y.(2003). Simulation of ship-bridge head-on collision based on finite element model of whole ship-bridge, Engineering Mechanics, 20: 5, pp.155-162.

LR(2000). Lloyd's Register of Shipping World Casualty Statistics 1996-1999.

LS-DYNA(2003). LS-DYNA Keyword Manual 970.Livermore Software Technology Corporation.

Marco A., Castelletti L. & Maurizio T.(2005). Fluid-structure interaction of water filled tanks during the impact with the ground, International Journal of Impact Engineering, vol. 31, pp.235-254.

Mcdermott J. F., Kline R.G., Jones E.L., et al.(1974). Tanker structural analysis for minor collisions. SNAME, 82: pp.229-414.

Minorsky V. U.(1959). An analysis of ship collisions with reference to protection of nuclear power plants. Journal of Ship Research, Vol.3 (Oct.): 1-4.

Mizukami M., Masayuki T., Nagahama S. & Kamei S.(1996). Collision simulation of a double hulled structure with uni-directional girder system. Proceedings, 6th International Offshore and Polar Engineering Conference, Los Angeles.

Motora S., Fujino M., et al.(1969). Equivalent Added Mass of Ships in Collisions. JSNA. Japan, 126 (Dec.): pp.141-152.

Nolau Neto J. A., Estefen S. F. & Quaranta F.(2004). Floating protection system for collision of supply vessel on FPSO hull, International Symposium on Practical Design of Ships and Other Floating Structures (PRADS), Luebeck-Travemuende, Germany, pp.12-17, September 2004.

Oh M., Kim J. H., Jang Y. S. & Bird E.(2005). Impact analysis of Greater Plutonio FPSO considering ship collision, International Offshore and Polar Engineering Conference (ISOPE),Seoul, Korea, pp.19-24, June 2005.

Ohtsubo H. & Suzuki K.(1994) The crushing mechanics of bow structure in head-on collision (1st report). Journal of the Society of Naval Architects of Japan, Vol.176, pp.301-308 (in Japanese).

Ohtsubo H. & Suzuki K.(1995). The crushing mechanics of bow structure and its optimal design against head on collision, Proceedings of PRADS'95, 2, pp.1060-1071.

Ohtsubo H. & Wang G.(1995). An upper bound solution to the problem of plate tearing, Journal of Marine Science and Technology, 1, pp.46-51.

Okazawa S., Fujikubo M. & Hiroi S.(2004). Static and dynamic necking analysis of steel plates in tension, International Conference on Collision and Grounding of Ships (ICCGS), Izu, Japan.

Ozguc O., Samuelides M. & Das P. K.(2005). A comparative study on the collision resistance of single and double side skin bulk carriers, International Congress of International Marinetime Association of the Mediterranean (IMAM), Lisboa, Portugal, pp.26–30.

Paik J. K.(1994). Cutting of a longitudinally stiffened plate by a wedge, Journal of Ship Research, 38:4, pp.340-348.

Paik J. K. & Pedersen P. T.(1995). Ultimate and crushing strength of plated structures. Journal of Ship Research, 39,3,Sept., pp.250-261.

Paik J. K. & Pedersen P. T.(1996). Modelling of the internal mechanics in ship collisions, Ocean Engineering, 23, pp.107-142.

Paik J. K. & Pedersen P. T.(1997). Simple assessment of post-grounding loads and strength of ships, International Journal of Offshore and Polar Engineering, 7:2, pp.141-145.

Paik J. K. & Thayamballi A. K.(2002). Ultimate limit state design of steel-plated structures, John Wiley & Sons, Chichester, U.K.

Paik J. K. & Wierzbicki T.(1997). A benchmark study on crushing and cutting of plated structures, Journal of Ship Research, 41:2, pp.147-160.

Paik J. K., Choe I. H. & Thayamballi A. K.(2002). Predicting resistance of spherical-type LNG carrier structures to ship collisions, Marine Technology, 39:2, pp.86-94.

Paik J. K., Chung J. Y. & Chun M. S.(1996). On quasi-static crushing of a stiffened square tube. Journal of Ship Research, 40, 3, Sept., pp.31-60.

Paik J. K., Chung J. Y., Choe I. H., Thayamballi A. K., Pedersen P. T. & Wang G.(1999). On rational design of double hull tanker structures against collision, Annual Meeting of the Society of Naval Architects and Marine Engineers (SNAME), Baltimore, MA.

Paik J. K., Wang G., Kim B. J. & Thayamballi A. K.(2002). Ultimate limit state design of ship hulls, SNAME Transactions, 110.

Petersen M. J.(1982). Dynamics of ship collision. Ocean Engineering, Vol. 9, No.4, pp.295-329.

Pedersen P. T.(1994). Ship grounding and hull-girder strength, Marine Structures, 7, pp.1-29.

Pedersen P. T.(1995). Collision and grounding mechanics, Proceedings of WEGEMT'95, Copenhagen, 1, pp.125-157.

Pedersen P. T., Gluver H. & Dosen D.(1998). Proceedings of the International Symposium on Advances in Ship Collision Analysis, Copenhagen, Denmark, Ed., A.A. Balkema, Rotterdam, the Netherlands.

Pedersen P. T, Valsgard S., Olsen D. & Spangenberg S.(1993). Ship impacts: bow collisions, International Journal of Impact Engineering, 13, pp.163-187.

Pedersen P. T. & Zhang S.(1998). On impact mechanics in ship collisions, Marine Structures, 11:10, pp.429-449.

Pedersen P. T. & Zhang S.(2000). Absorbed energy in ship collision and grounding – revising Minorsky's empirical method, Journal of Ship Research, Vol. 44, No.2, pp.40-154.

Pierre C. Sames, Delphine Marcouly & Thomas E. Schellin(2002). Sloshing in rectangular and cylindrical tanks, Journal of Ship Research, vol. 46, No. 3, pp.186-200.

Radovitzky R. & Ortiz M.(1998). Lagrangian finite element analysis of Newtonian fluid flows, International Journal for Numerical Methods in Engineering, vol 43, pp.607-619.

Reich M. & Rohr U.(2004). A hybrid computational model for ship grounding, Schiffstechnik (Ship Technology Research), 52.

Sandia National Laboratories (1998), Data and methods for the assessment of the risks associated with the maritime transport of radioactive materials results of the SeaRAM program studies, SAND98-1171/2, Albuquerque, NM

Servis D. & Samuelides M.(2000). Ship collision analysis using finite elements. IASS-IACM 2000, 4th International Colloquium on Computation of Shell & Spatial Structures. Chania-Greece.

Servis D., Samuelides M., Louka T. & Voudouris G.(2002). Implementation of Finite-Element Codes for the Simulation of Ship-Ship Collisions Journal of Ship Research, Vol. 46, No. 4, pp.239–247.

Simonsen B. C.(2000). Bottom raking damage of high speed craft, Trans. RINA, 142, pp.41-58.

Simonsen B. C. & Lauridsen L. P.(2000). Energy absorption and ductile fracture in metal sheets under lateral indentation by a sphere, International Journal of Impact Engineering, 24, pp.1017-1039.

Simonsen B. C. & Pedersen P. T.(1995). Analysis of ship groundings on soft sea beds, Proceedings of PRADS'95, Seoul, 2, pp.1096-1109.

Simonsen B. C. & Törnqvist R.(2004). Experimental and numerical modeling of ductile crack propagation in large-scale shell structures, Journal of Marine Structures, 17, pp.1-27.

Simonsen B. C. & Törnqvist R.(2004). A formula for prediction of grounding damage with application to damage stability safety. 3rd International Conference on Collision and Grounding of Ships (ICCGS). 25-27 October 2004, Izu, Japan.

Simonsen B. C., Lutzen M. & Törnqvist R.(2004). MCA Research Project 501: HSC raking damage (Prepared for Maritime Coastguard Agency, UK), Nos. 1 to 5, April 2004.

Souli M., Ouahsine A. & Lewin L.(2000). ALE formulation for fluid-structure interaction problems, Computer methods in applied mechanics and engineering, Vol 190, pp.659-675.

Souli M., Olovsson L. & Do I.(2002). ALE and fluid/structure interaction capabilities in LS-DYNA. 7th International LS-DYNA Users Conference, Michigan, pp.1027-1036.

Suzuki K., Ohtsubo H. & Saiji K. S.(2000). Evaluation method of absorbed energy in collision of ships with anti-collision structure, Ship Structure Symposium, Arlington, VA.

Suzuki K., Ohtsubo H. & Saiji K. S.(2001). A simplified internal and external mechanics model for ship's collision, International Symposium on Practical Design of Ships and Mobil Units (PRADS), 1301-1307, Shanghai, China.

Tabri K., Broekhuijsen J., Matusiak J. & Varsta P.(2004). Analytical modelling of Ship Collision Based on Full Scale Experiments. 3rd International Conference on Collision and Grounding of Ships (ICCGS 2004), Izu, Japan, pp.302-311.

Tagg R., Bartzis P., Papanikolaou A., Spyrou K. & Lützen M.(2001). Updated vertical extent of collision damage, Proceedings of ICCGS'01, pp.101-113.

Tasai F.(1961). Hydrodynamic Force and moment produced by swaying and rolling oscillation of cylinders on the free surface, Reports of Research Institute for Applied Mechanics, Vol. IX, No 35.

Tikka K. K.(2001). Prediction of structural response in grounding application to structural design, SSC-417, Ship Structure Committee.

Thomas P. F.(1992). Application of plate cutting mechanics to damage prediction in ship grounding, MIT-industry joint program on tanker safety, Report No.8.

Törnqvist R. & Simonsen B. C.(2004). Safety and structural crashworthiness of ship structures: Modelling tools and application in design, International Conference on Collision and Grounding of Ships (ICCGS), Izu, Japan, 25-27 October 2004.

Törnqvist R.(2003). Design of Crashworthy Ship Structures, PhD Thesis, Technical University of Denmark, Lyngby, Denmark.

Urban J.(2003). Crushing and Fracture of Lightweight Structures, PhD Thesis, Technical University of Denmark, Lyngby, Denmark.

USCG (1991). USCG Ship Casualty Data, 1982-1990

Vredeveledt A. W., Wevers L. J. & Lemmen P. P. M.(1993). Full scale collision tests. 3rd International Symposium on Structural Crashworthiness and Failure, Liverpool.

Wang G.(1995). Structural analysis of ships' collision and grounding. PhD thesis, The University of Tokyo, December.

Wang G.(2002). Some recent studies on plastic behaviour of plates subjected to very large load, Journal of Ocean Mechanics and Arctic Engineering, ASME, 124:3, pp.125-131.

Wang G. & Ohtsubo H.(1997). Deformation of ship plate subjected to very large load, Proceedings of the 16th International Conference on Offshore Mechanics and Arctic Engineering (OMAE'97), Yokohama, 2, pp.173-180.

Wang G. & Ohtsubo H.(1999). Impact load of a supply vessel, Proceedings of ISOPE'99, Brest,France, 4, pp.463-471.

Wang G., Arita H. & Liu D.(2000). Behaviour of a double hull in a variety of stranding or collision scenarios, Marine Structures, 13, pp.147-187.

Wang G., Chen Y., Zhang H. & Peng H.(2002). Longitudinal strength of ships with accidental damages, Journal of Marine Structures, 15, pp.119-138.

Wang G., Ohtsubo H. & Arita K.(1998a). Large deflection of a rigid-plastic circular plate pressed by a rigid sphere, Journal of Applied Mechanics, 65, pp.533-535.

Wang G., Ohtsubo H. & Arita K.(1998b). Inner dynamics of side collision to bridge piers, In: Ship Collision Analysis, Balkema, Rotterdam, pp.53-60.

Wang G. Ohtsubo H. & Liu D.(1997). A simple method for predicting the grounding strength of ships, Journal of Ship Research, 41:3, pp.241-247.

Wang G., Seah A. K. & Shin Y. S.(2002). Predicting ship structure performance in accidents, Proceedings of MARTECH'2002, Singapore Polytechnic Institute, September, Singapore.

Wang G., Spencer J. & Chen Y. J.(2002). Assessment of ship's performance in accidents, Journal of Marine Structures, 15, pp.313-333.

Wang K. & Yi Y.(1997). Study on the protective design of bridge pier (in Chinese), Journal of Hebei University of Technology, 26: 4, pp.37 – 44.

Wierzbicki T.(1995). Concertina tearing of metal plates, International Journal of Solid Structures, 19, pp.2923-2943.

Wierzbicki T. & Abramowicz W.(1983). On the crushing mechanics of thin-walled structures, Journal of Applied Mechanics, ASME, 50, pp.727-734.

Wierzbicki T. & Thomas P.(1993). Closed-form solution for wedge cutting force through thin metal sheets, International Journal of Mechanical Sciences, 35, pp.209-229.

Wierzbicki T., Peer D. B. & Rady E.(1993). The anatomy of tanker grounding, Marine Technology, 30:2, pp.71-78.

Woisin G.(1979). Design against collision, Proceeding of International Symposium on Advances in Marine Technology, pp.309-336.

Woisin G.(1998). Analysis of the collision between rigid bulb and side shell panel, Proceedings of PRADS'98, The Hague, pp.165-172.

Woisin G.(1999). Discussion on Kitamura (1997). "Comparative study on collision resistance of side structure", Marine Technology, 36:4, pp.228-231.

Wu F., Spong R. & Wang G.(2004). Using Numerical Simulation to Analyze Ship Collision. The three International Conference on Collision and Grounding of Ships. Izu, Japan, October pp.27-33.

Yamada Y. & Endo H.(2004). Collapse strength of the buffer bow structure in oblique collision. 3rd International Conference on Collision and Grounding of Ships (ICCGS 2004), 160-171, Izu, Japan, 25-27 October 2004.

Yamada Y., Endo H. & Pedersen P. T.(2005). Numerical study on the effect of buffer bow structure in ship-to-ship collisions, International Offshore and Polar Engineering Conference (ISOPE), Seoul, Korea, 19-24 June 2005.

Yang P. D. C. & Caldwell J. B.(1988). Collision energy absorption of ships. bow structures. International Journal of Impact Engineering, 7:2, pp.181-196.

Yu X.(1996). Structural analysis with large deformations until fracture and with dynamic failure, Dr. Thesis, Hamburg University (in German).

Zhang H., Wu S. & Chen T.(1990). Analysis on the strength of double-sided shipside (in Chinese), Shipbuilding of China, 108:2, pp.51 - 60.

Zhang L., Egge E. & Bruhns H.(2004). Approval Procedure Concept for Alternative Arrangements The three International Conference on Collision and Grounding of Ships. Izu, Japan, October pp.87-96.

Zhang S.(1999). The Mechanics of Ship Collisions, PhD Thesis, Technical University of Denmark, Lyngby, Denmark.

Zhang S.(2002). Plate tearing and bottom damage in ship grounding, Marine Structures, 15, pp.101-107.

Zhang S., Ocakli H. & Pedersen P.T.(2004). Crushing of ship bows in head-on collision, International Journal of Maritime Engineering, Transactions of the Royal Institution of Naval Architects, 146: A2, pp.39-46.

Zhu L.(1990). Dynamic inelastic behaviour of ship plates in collision, Ph.D. Thesis, Department of Naval Architecture and Ocean Engineering, University of Glasgow, Glasgow.

Zhu L. & Atkins A. G.(1998). Failure criteria for ship collision and grounding, Proceedings of PRADS'98, The Hague, pp.141-148.

Zhu H., Zheng J. & Liu S.(1996). Comparison between the strength of one-sided shipside and doublesided shipside (in Chinese), Journal of Huazhong University of Technology, 24:1, pp.75-78.